AD-A054 342 ROCKWELL INTERNATIONAL THOUSAND OAKS CALIF SCIENCE --ETC F/G 11/2
HIGH TEMPERATURE MECHANICAL PROPERTIES OF POLYPHASE CERAMICS BA--ETC(U)
MAR 78 F F LANGE F49620-77-C-0072

UNCLASSIFIED SC5099.1IR AFOSR-TR-78-0943 NL

| OF
AD
A054 342

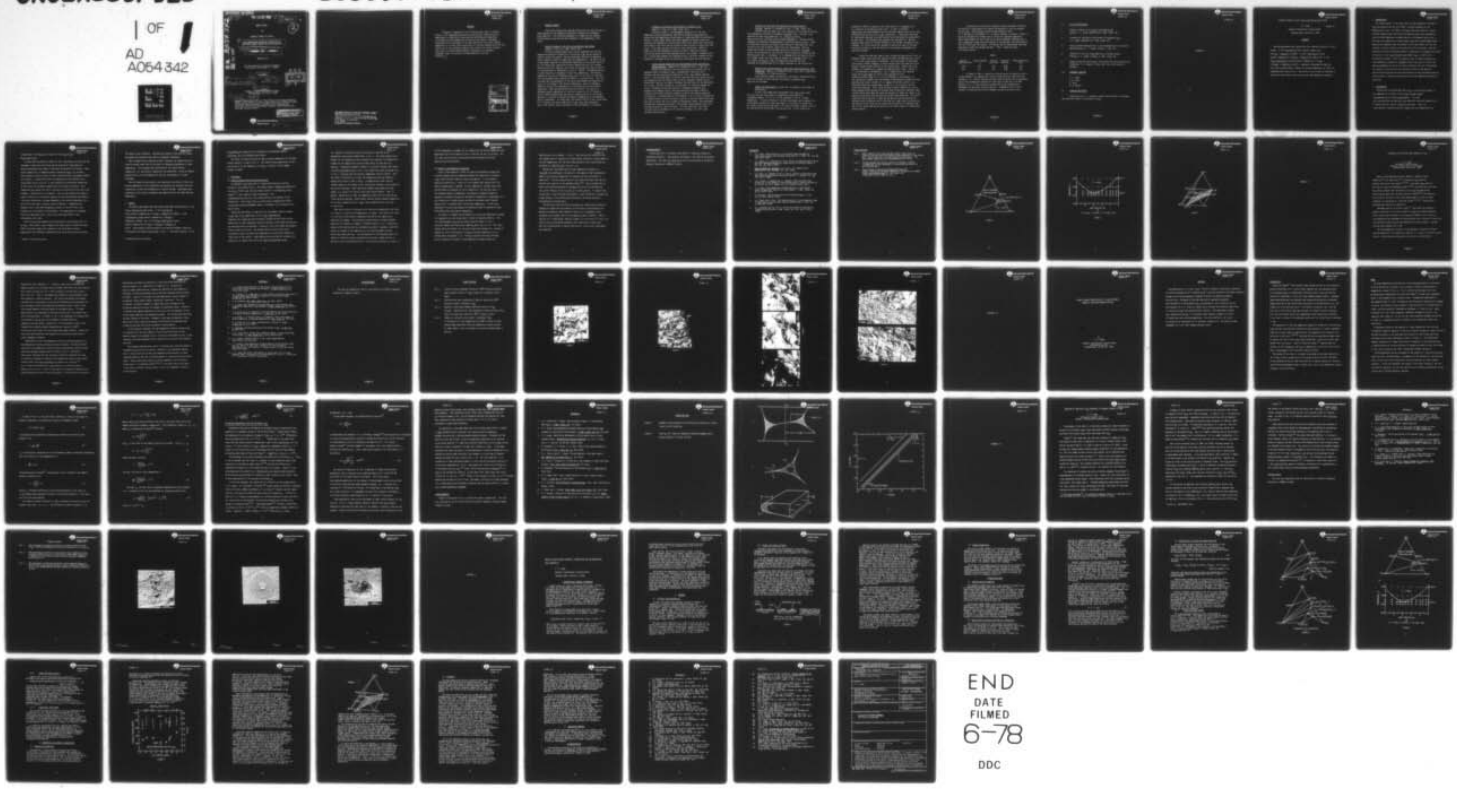

END
DATE
FILMED
6-78
DDC

SC5099.1IR

4

ANNUAL REPORT

ON

CONTRACT F49620-77-C-0072

HIGH TEMPERATURE MECHANICAL PROPERTIES OF POLYPHASE CERAMICS BASED ON SILICON NITRIDE

Annual rept.
1 Feb [redacted] 77 - 31 Jan [redacted] 78,

Submitted to

Air Force Office of Scientific Research
Bolling Air Force Base, D. C. 20332

March 1978

F49620-77-C-0072

By 77 p.

F. F. Lange
Rockwell International Science Center
Thousand Oaks, California 91360

2306 A2

"Research sponsored by the Air Force Office of Scientific Research (AFSC), United States Air Force, under Contract No. F49620-77-C-0072. The United States Government is authorized to reproduce and distribute reprints for governmental purposes notwithstanding any copyright notation hereon."

Rockwell International, Thousand Oaks, CA.
Science Center

389 949

AIR FORCE OFFICE OF SCIENTIFIC RESEARCH (AFSC)
NOTICE OF TRANSMITTAL TO DDC
This technical report has been reviewed and is approved for public release IAW AFR 190-12 (7b).
Distribution is unlimited.
A. D. BLOSE
Technical Information Officer

ABSTRACT

Progress is summarized in the following study areas: (1) eutectic studies in the Si_3N_4-MgO-SiO_2 system relating eutectic compositions and temperatures to fabrication, microstructure and mechanical properties; (2) evidence for high temperature cavitation crack growth in polyphase Si_3N_4 materials; (3) estimates of the time required for the stress induced penetration of a liquid from triple points to locations between grains; (4) the reaction of Fe with polyphase Si_3N_4 to form surface pits during oxidation which lead to strength degradation, (5) creep behavior of polyphase Si_3N_4/MgO alloys in relation to the MgO/SiO_2 molar ratio and cavitation.

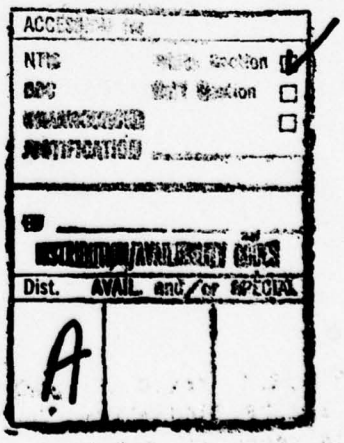

I. PROGRESS SUMMARY

Significant progress has been made during the last contract year in understanding the high temperature mechanical properties of polyphase Si_3N_4 materials. The following paragraphs will summarize this progress with reference to the detailed work presented in the appendices of this report.

Eutectic Studies in the Si_3N_4-Si_2N_2O-Mg_2SiO_4-MgO System:
Appendix I (Sub. to J. Amer. Ceram. Soc.)

Previous strength/compositional results suggested that the high temperature mechanical properties of hot-pressed Si_3N_4 may be related to eutectics within the system. Melting experiments were used to determine several important eutectic compositions and temperatures. The effect of CaO (a detrimental impurity) on the melting temperature of the ternary eutectic was also determined, showing that certain compositions with this system, containing CaO as an impurity, can contain an equilibrium liquid as part of its microstructure at temperatures as low as ~1325°C. The combined effect of other impurities is expected to lower this temperature. The eutectic composition occurred at a MgO/SiO_2 molar ratio of 1.6, which is coincident with the strength minima observed at 1400°C in a previous study. This work concluded that the degradation of the sub-solidus mechanical properties of Si_3N_4 will be related to the eutectic temperature. When all secondary phases are crystalline, degradation will be precipitous at the eutectic temperature. When non-equilibrium conditions prevail (the case of an amorphous phase), degradation will not be as rapid, but it will begin at several hundred degrees below the eutectic temperature due to the gradual decrease in viscosity as the melting eutectic temperatures of the amorphous phase is approached. In either case, the volume fraction of the viscous phase will increase as the gross composition (Si_3N_4, SiO_2, MgO) approaches that of the eutectic and/or the amount of the CaO impurity is increased.

Evidence for Cavitation Crack Growth in Polyphase Si_3N_4: Appendix II (Sub. to J. Amer. Ceram. Soc.)

Slow-crack growth is the phenomenon responsible for the high temperature strength degradation exhibited by polyphase Si_3N_4 materials. Because the high temperature microstructure of these materials are believed to contain a viscous phase, models have been suggested to explain slow-crack growth by the formation of cavities within the viscous phase within the stress field ahead of the crack and the linking of these cavities to cause slow crack growth. This model has been verified by direct observation. Material underlying the high temperature fracture surface is observed to contain cavities and grains which had separated during crack growth. Evidence exists for a viscous phase between the separated grains, and direct evidence for the extension of secondary cracks by cavitation crack growth was also obtained.

Stress Induced Penetration of Liquid Between Grains by Solution - Reprecipitation: Appendix III (accepted for pub., J. Mat. Sci.)

Recent high resolution electron microscopy has indicated that the amorphous phase in polyphase Si_3N_4 is predominantly located at grain junctions and only occasionally observed as a thin layer between adjacent grains. Since existing models to explain creep and slow-crack growth relie on the assumption that the viscous phase initially separates adjacent grains, a theoretical study was initiated to estimate the conditions for the penetration of a liquid, initially located at a triple point, to locations between the grains. Estimates of the time required to completely penetrate grain boundaries was modeled using a solution-reprecipitation mode of material transport and fracture mechanics concepts to derive the chemical potential driving force. Diffusion data for the transport of Si in liquid silicates and the Stokes-Einstein relation relating viscosity to diffusion coefficients were both used to derive the flux of material through the liquid. Both approaches estimate short penetration periods ($\sim$30 seconds) under moderate stress near the melting point of liquid silicates. For such conditions, the liquid silicates can be considered for all practical purposes, as a thin layer between adjacent grains.

Reaction of Iron with Si_3N_4 Materials to produce Surface Pitting: Appendix IV (accepted for pub., J. Amer. Ceram. Soc.)

Previous work had shown that large surface pits are formed during the high temperature oxidation of polyphase Si_3N_4/MgO alloys. Pitting is not observed for other Si_3N_4 materials, e.g., Si_3N_4/Y_2O_3 alloys. These surface pits can cause severe strength degradation. Surface pitting suggested the presence of heterogeneously distributed reactive sites. Since Fe containing inclusions are found on the surface of these materials, the reaction of Fe with different Si_3N_4 alloys was investigated. Results showed that surface pitting produced during the oxidation of Si_3N_4/MgO alloys can be caused by Fe, and that the reactivity/pitting increases as the MgO/SiO_2 molar ratio is increased. It is presumed that the reaction of FeO (or a higher oxide) with the oxidation products of Si_3N_4/MgO alloys, viz. SiO_2, $MgSiO_3$ and Mg_2SiO_4 forms low temperature eutectics and thus increases at oxidation/reactivity at these locations to form surface pits.

Dense Silicon Nitride Ceramics: Fabrication and Interrelation with Properties: Appendix V (accepted for pub., cont. Proc., Fabrication of Ceramics, N.C. State University)

Interrelations between raw materials, fabrication, phase equilibria, mechanical properties and oxidation resistance of polyphase Si_3N_4 materials was reviewed.

Summary of Creep Results (current work in progress, not written for publication)

An axial high temperature extensometer with Si_3N_4 cross pieces and Al_2O_3 rods was constructed for compressive creep testing of rectangular (Approx. 0.3 x 0.3 x 1.0 cm) specimens in air at elevated temperatures. A linear differential variable transformer was to measure the displacements between the Si_3N_4 cross beams to an accuracy of $\pm$0.0002 cm. An Instron testing machine was used in its load cycle mode to apply a load to the specimen which cycled $\pm$3% of the desired load. Initial testing was

performed at 1400°C to determine the creep behavior of Si_3N_4/MgO alloys as a function of the MgO/SiO_2 molar ratio. To date, 6 different compositions have been examined from two different compositional series, each containing 83.5 M/o and 75 M/o Si_3N_4, respectively. Testing was performed by loading each specimen to various stress levels and obtaining steady-state at each level. Two specimens were examined for each material. Behavior between stress levels of 175 MPa (25,000 psi) and 700 MPa (100,000 psi) was examined. An initial period was consumed in working out many of the bugs associated, primarily, with the function of the ceramic extensometer and specimen alignment.

Results to date have lead to many interesting observations: First, as expected, higher creep rates are obtained as either the MgO/SiO_2 molar ratio $\rightarrow$ 2 or as the Si_3N_4 content is decreased. This observation is consistent with eutectic studies (Appendix I) which indicate that such materials should contain a higher volume fraction of the viscous phase. Second, the stress exponent (n) systematically changes with MgO/SiO_2 molar ratio. Values of $n \sim 1$ are obtained as the MgO/$SiO_2 \rightarrow 0$ or ∞ (compositions that approach either the Si_3N_4-Si_2N_2O tie line or the Si_3N_4-MgO tie line, respectively) and values of $n = 1.5$-2 are obtained as the MgO/$SiO_2 \rightarrow 2$. This observation suggests that the dominant creep mechanism changes with the MgO/SiO_2 molar ratio, (values of $n \sim 1$ suggest diffusional control, e.g., diffusion within the viscous phase; values of $n \rightarrow 2$, currently, have no theoretical meaning). Third, large residual stresses (opposite in sign to those imposed during testing) are present upon unloading the specimen, these residual stress decay away and cause the specimen to change its length in the opposite direction as that observed during the creep experiment. This third observation was evident by a) removing the applied load and watching the specimen reload the machine and b) unloading to a lower stress and observing the residual stress decay as the creep curve returned to its expected form. The first of these observations would not have been evident in a dead-weight testing machine.

A high precision sink-float technique has been developed to measure the density of Si_3N_4 materials to detect the presence of cavities produced during creep. The technique involves mixing methylene iodine (ρ = 3.325 gm/cc) and neothane (ρ = 1.3 gm/cc) together to produce a liquid in which the specimen will neither sink ncr float at a measured temperature. Density measurements of the liquids by the usual pycnometer technique over a small temperature range allows the density of the specimen to be determined to the third place past the decimal. Preliminary density measurements have been performed on crept and uncrept specimens. Table I summarizes these preliminary results.

TABLE I

Material (MgO/SiO_2 Ratio	Stress Exponent n	% Strain After Test	% Density Decrease	% Density/% Strain Ratio
0.25	0.8	2.3	0.24	0.1
1.7	1.6	2.4	1.65	0.7
5.0	1.1	3.3	0.62	0.2

As shown in Table I, exensive cavitation occurs for materials with a stress exponent >1.5, whereas very little cavitation occurs when the stress exponent is ~1. Current thinking indicates that cavitation (grain separation) may be the accommodation mechanism for one group of materials (viz when $MgO/SiO_2 \rightarrow 2$, $n \sim 2$) and diffusional process may be the accommodating phenomenon for the other group of materials. Systematic work is now in progress to determine the relation between cavitation and strain rate.

II. LIST OF PUBLICATIONS

1. "Eutectic Studies in the Si_3N_4-Si_2N_2O-Mg_2SiO_4-MgO System," F. F. Lange, Submitted to J. Amer. Ceram. Soc.

2. "Evidence for Cavitation Crack Growth in Polyphase Si_3N_4," F. F. Lange, submitted to J. Amer. Ceram. Soc.

3. "Stress Induced Penetration of a Liquid Between Grains by Solution - Reprecipitation," F. F. Lange, in press, J. Mat. Sci.

4. "Reaction of Iron with Si_3N_4 Materials to Produce Surface Pitting," F. F. Lange, in press, J. Amer. Ceram. Soc.

5. "Dense Silicon Nitride Ceramics: Fabrication and Interrelations with Properties," F. F. Lange, in Press, Conf. Proc. Fabrication of Ceramics.

III. PERSONNEL INVOLVED

F. F. Lange
A. G. Evans
B. Davis
M. G. Metcalf

IV. COUPLING ACTIVITIES

Discussions with L. J. Gauckler of Max Plunk Institute in Stuttgart have been most helpful in the eutectic study.

APPENDIX I

Rockwell International
Science Center

EUTECTIC STUDIES IN THE Si_3N_4-Si_2N_2O-Mg_2SiO_4-MgO SYSTEM

F.F. Lange

SC5099.1IR

Rockwell International Science Center

Thousand Oaks, California 91360

ABSTRACT

Melting experiments have established three important eutectics in this system: 1) the Si_3N_4-Mg_2SiO_4 binary eutectic composition, $0.2Si_3N_4 + 0.8Mg_2SiO_4$ at 1560°C, 2) the Si_2N_2O-Mg_2SiO_4 binary eutectic composition, $0.4Si_2N_2O + 0.6Mg_2SiO_4$ at 1525°C, and 3) the Si_3N_4-Si_2N_2O-Mg_2SiO_4 ternary eutectic composition, $0.1Si_3N_4 + 0.3Si_2N_2O + 0.6Mg_2SiO_4$ at 1515°C. Systematic replacement of MgO with CaO in the ternary eutectic reduced its melting temperature to 1325°C for a MgO/CaO molar ratio of 0.67. The results of this study are discussed in relation to fabrication, microstructure and high temperature strengths.

1. INTRODUCTION

In a recent paper,[1] it was shown that the high temperature strength of Si_3N_4 hot-pressed with the aid of MgO is strongly dependent on the MgO/SiO_2 molar ratio. At 1400°C, strength minima were observed in three different compositional series when the MgO/SiO_2 molar ratio approached 2. Since the high temperature strength behavior of polyphase Si_3N_4 alloys is believed to be governed by a liquid phase, these new strength-compositional observations suggested that the content of the liquid phase, and thus the strength, should be related to the eutectics within the system. Work was therefore initiated to determine eutectic compositions and temperatures within the portion of the Si_3N_4-SiO_2-MgO system where Si_3N_4 is known to be an equilibrium phase.[1] Since the impurity, CaO, is known to degrade the high temperature strength of Si_3N_4/MgO alloys,[2] the effect of CaO on the melting temperature of one of the ternary eutectics was also investigated. The results of this work will be discussed in terms of the expected equilibrium and non-equilibrium microstructures of these polyphase materials and the effect of these microstructures on the high temperature mechanical properties.

2. EXPERIMENTAL

Previous work had established that Si_3N_4 is an equilibrium phase in two compatability triangles of the Si_3N_4-SiO_2-MgO system:[1] Si_3N_4-MgO-Mg_2SiO_4 and Si_3N_4-Si_2N_2O-Mg_2SiO_4. This work also indicated that the eutectics associated with these two compatibility triangles might be close to th Mg_2SiO_4 end member. Thus, the investigation to determine eutectic compositions and temperatures was

concentrated in the Mg_2SiO_4 rich region of the Si_3N_4-Si_2N_2O-Mg_2SiO_4-MgO system.

A carbon heating system was chosen for this investigation to duplicate the atmoshperic conditions used during the hot-pressing of Si_3N_4 materials. Melting experiments were chosen to determine the eutectics of interest. Seven master compositions of composite powders containing Si_3N_4, SiO_2 and MgO were prepared by liquid milling in plastic bottles containing tungsten carbide milling media. Compositions within the compositional area defined by the seven master batches (see Fig. 1) were prepared by mixing proper proportions of two or more of the master compositions with a morter and pestle. Each composition was pressed into one of an array of blind holes drilled into a 5cm diameter, 1.25cm thick disc of graphite. The disc was covered with graphite paper*, placed with a cylindrical graphite die with end-plungers and heated in a hot-press containing a nitrogen atmosphere to the desired temperature for a period of 30 min under a uniaxial stress of 2000 psi. Temperature was measured with a Pt/Pt-10Rh thermocouple placed in a hole drilled in the graphite die to the depth of the specimens. The thermocouple was rebeaded after each experiment, and it could not be used above 1600°C in the carbonaceous environment.

After cooling, each composition was examined for the characteristics of melting. Below 1500°C, molten compositions formed spherical beads and above 1500°C the molten compositions appeared to wet the graphite surface. Compositions which exhbited incomplete melting and/or densification retained

* Grafoil, Union Carbide Corp.

the shape of their container. Specimens and graphite discs were not reused; new powder and containers were used for subsequent experiments.

When a composition was observed to melt, adjacent, new compositions were mixed to replace those that did not melt for subsequent experiments at lower temperatures. This procedure was iterated until the lowest melting composition, viz. the eutectic composition, was determined. Using two stacked graphite discs, up to 46 compositions could be investigated in a single experiment.

Once the lowest ternary eutectic was determined, the effect of CaO on the melting temperature of this composition was determined by forming a series of compositions in which CaO systematically replaced the MgO. Experiments were conducted on this series to determine the composition with the lowest melting temperature.

3. RESULTS

The melting experiments described above established three eutectics in the Si_3N_4-Si_2N_2O-Mg_2SiO_4-MgO system: 1) the Si_3N_4-Mg_2SiO_4 binary eutectic composition*, $0.2Si_3N_4 + 0.8Mg_2SiO_4$ at 1560°C, 2) the Si_2N_2O-Mg_2SiO_4 binary eutectic composition, $0.4Si_2N_2O + 0.6Mg_2SiO_4$ at 1525°C, and 3) the Si_3N_4-Si_2N_2O-Mg_2SiO_4 ternary eutectic composition, $0.1Si_3N_4 + 0.3Si_2N_2O + 0.6Mg_2SiO_2$ at 1515°C. These eutectics and the extent of the observed boundary curves are illustrated on the phase diagram shown in Fig. 1. The ternary eutectic in the

* Expressed as mole fractions

Si_3N_4-MgO-Mg_2SiO_4 compatibility triangle was not determined because experiments were not conducted above 1600°C.

The effect of substituting CaO for MgO on melting temperature of the known ternary eutectic is shown in Fig. 2. The lowest melting composition in this series occurs for the composition $0.11Si_3N_4 + 0.34SiO_2 + 0.55$ (0.4MgO + 0.6CaO) at 1325°C.

4. DISCUSSION

4.1 Eutectics, Densification and Microstructure

As expected, Si_3N_4 takes part in a generalized reaction with SiO_2 and MgO to form eutectic melts. The ternary eutectic temperature observed in this work is ~50°C lower than the lowest eutectic in the MgO-SiO_2 binary system.[3,4] Lower eutectics might be expected in the Si_2N_2O-$MgSiO_4$-SiO_2 portion of the system which was not explored in the present work. Since Si_3N_4 alloys are fabricated at temperatures >1650°C, liquid phase sintering phenomena appear, as expected, to be responsible for densification.

Neglecting the effects of impurities for the moment, composite powder (Si_3N_4, MgO, SiO_2) compositions in the Si_3N_4-Si_2N_2O-Mg_2SiO_4 compatibility triangle may form transient, non-equilibrium liquids during heating due to lower temperature eutectics outside of the system studied here, but once equilibrium is obtained, a liquid will only exist above the system's ternery eutectic of 1515°C. the volume fraction of the liquid can be increased by either increasing the temperature or shifting the composition toward that of the eutectic. When impurities such as CaO are included, the composition no longer rests within the Si_3N_4-SiO_2-Mg_3N_2-MgO system,

viz. reactions including CaO must be considered as depicted by the hypothetical equivalence diagram shown in Fig. 3. The shaded compositional element in this hypothetical phase diagram could represent the compatibility element for the compositions discussed above which includes CaO as an impurity. Although the element's eutectic is presently unknown, the results of melting experiments shown in Fig. 2 for composition along the broken line in Fig. 3 illustrate that the eutectic temperature could be <1325°C. Thus, the effect of CaO would be to lower the temperature where the composite powders would react to form a liquid. At temperatures higher than the element's eutectic, the content of the liquid would increase as the content of the CaO was increased. Other impurities commonly associated with Si_3N_4 powder, e.g. oxides of Al and Fe, could have similar effects. Thus, in general, impurities will lower the temperature where the first equilibrium liquid would be observed. Densification kinetics should therefore depend not only on gross composition (e.g. Si_3N_4. SiO_2 and MgO contents), but also on impurities.

When densification is achieved at the fabrication temperature, the liquid will begin to solidify as the temperature is lowered. The last bit of liquid will solidify at the eutectic temperature defined by the composition's compatibility element. The sub-solidus microstructure of these polyphase materials will depend on a number of different factors, e.g. if crystalline phases solidify during cooling, the amount and type of secondary crystalline phases will depend on the composition of the starting powders and the sub-solidus phase relations. The configuration of the secondary phases will depend on interfacial energy considerations and their volume fraction as defined by rules of phase equilibria. If the liquid solidifies as a glass, it

is not unreasonable to suggest tht its composition and melting temperature may approximate that of the eutectic since it would be the last to solidify. For this case, the sub-solidus microstructure would represent the frozen, super-solidus microstructure.

4.2 Eutectics and Mechanical Properties

Since a liquid phase will alter all sub-solidus mechanical properties, relations between the high temperature mechanical properties of polyphase Si_3N_4 alloys and their eutectics should be expected. If the secondary phases are crystalline, a liquid will not reappear upon heating until the eutectic temperature is reached. At this temperature, strength should fall precipitiously as observed for SiC-Si composites.[5] On the other hand, if the secondary phases are amorphous, the mechanical properties might be expected to gradually decrease as the eutectic temperature is approached, vis. the viscousity of silcate glasses can begin to decrease several hundred degrees prior to reaching their true melting temperature. In this case, degradation of sub-solidus mechanical properties might be expected to begin 100°C-300°C below the eutectic temperature.

The effects of composition and impurities on the high temperature strength of Si_3N_4/MgO alloys can be explained in terms of observed eutectics. The line drawn between Si_3N_4 and the ternary eutectic shown in Fig. 2 describes compositions containing a MgO/SiO_2 molar ratio of 1.6. The liquid content above the eutectic (or the sub-solidus glass content) for a series of composition with a fixed amount of Si_3N_4 but variable MgO/SiO_2 will be a maximum where the MgO/SiO = 1.6. Previous studies[1] with three different series of materials resulted in high temperature strength minima at a

MgO/SiO_2 molar ratio between 1.5-2.0. These results are consistent with the argument that all materials with each series contained a viscous phase at the test temperature, and that the volume content of the viscous phase was maximized at a MgO/SiO_2 molar ratio of 1.6.

Stuides have also shown that the high temperature strength of a Si_3N_4/MgO alloy decreased in proportion to the amount of CaO intentionally added to the starting composition to simulate and study the effect of impurities.[2] Previous explanations for this effect have been that CaO will decrease the viscosity of the amorphous phase.[2,6,7] But as pointed out by Powell and Drew[8] and observed by Turkdogan and Bills,[9] CaO and MgO have very similar effects on the viscosity of silicate glasses. In light of the current work, a more consistent explanation is that the CaO will increase the volume content of the viscous phase according to the phase equilibria considerations discussed above.

The discussion resulting from the present work concerning the effect of composition, impurities and eutectics on fabrication, microstructure and mechanical properties should generally apply to all Si_3N_4/metal oxide polyphase alloy systems, and to all polyphase systems in general. When an impurity in a 'single-phase' material exceeds its solid-solubility limit, the material must be considered polyphase, which immediately invokes phase equilibria consierations to explain fabrication, microstructure development and properties.

ACKNOWLEDGEMENTS

Discussions with L.J. Gauckler were helpful in choosing a method for determining eutectics. The technical assistance of M.G. Metcalf was greatly appreciated. This work was supported by the Air Force Office of Scientific Research, Contract No. F49620-77-C-0072.

REFERENCES

1. F.F. Lange, "Phase Relations in the System Si_3N_4-SiO_2-MgO and Their Interrelation with Strength and Oxidation," J. Amer. Cer. Soc. 61, (102) 53-6 (1978).

2. J.L. Iskoe, F.F. Lange and E.S. Diaz, "Effect of Selected Impurities on the HIgh Temperature Mechanical Properties of Hot-Pressed Si_3N_4," J. Mat. Sci. 11, 908-12 (1976).

3. Phase Diagrams for Ceramists, E.M. Levin, C.R. Robbins and F. McMurdie, Fig. 266, The Amer. Cer. Soc. (1964).

4. F.R. Boyd, J.L. England and B.T.C. Davis, "Effects of Pressure on the Melting and Polymorphism of Enstatite, $MgSiO_3$," J. Geophys. Res. 69, (10) 2101-9 (1964).

5. C.W. Forrest, P. Kennedy and J.V. Shennan, "The Fabrication and Properties of Self-Bonded Silicon Carbide Bodies," Special Ceramics 5, pp. 99-123, ed. by P. Popper, B.C.R.A. Stoke-on-Trent (1972).

6. F.F. Lange, "High-Temperature Strength Behavior of Hot-Pressed Si_3N_4: Evidence for Subcritical Crack Growth," J. Amer. Ceram. Soc. 57 (2), 84-87 (1974).

7. R. Kossowsky, "The Microstructure of Hot-Pressed Si_3N_4," J. Mat. Sci. 8, (11), 1603-15 (1973).

8. B.D. Powell and P. Drew, "The Identification of a Grain-Boundary Phase in Hot-Pressed Si_3N_4 by Auger Electron Spectroscopy," J. Mat. Sci. 9, 1869-1870 (1974).

9. E.T. Turkdogan and P.M. Bills, "A Critical Review of Viscosity of CaO-MgO-Al_2O_3-SiO_2 Melts," Amer. Ceram. Soc. Bull. 39 (11) 682-7 (1960).

FIGURE CAPTIONS

Fig. 1 Phase diagram of the Si_3N_4-SiO_2-MgO system illustrating the eutectics and the extent of boundary curves determined in the present work. Sub-solidus tie lines were determined previously.[1] The seven master compositions are represented by full circle.

Fig. 2 The join between the ternary eutectic, $0.11Si_3N_4 + 0.34SiO_2 + 0.55MgO$ and its CaO counterpart, illustrating the results of melting experiments.

Fig. 3 Phase diagram of theSi_3N_4-SiO_2-Mg_3N_2-MgO-Ca_3N_2-CaO system illustrating the shaded hypothetical compatibility element Si_3N_4-Si_2N_2O-$CaMgSiO_4$-$MgSiO_4$. The broken line illustrates the join shown in Fig. 2

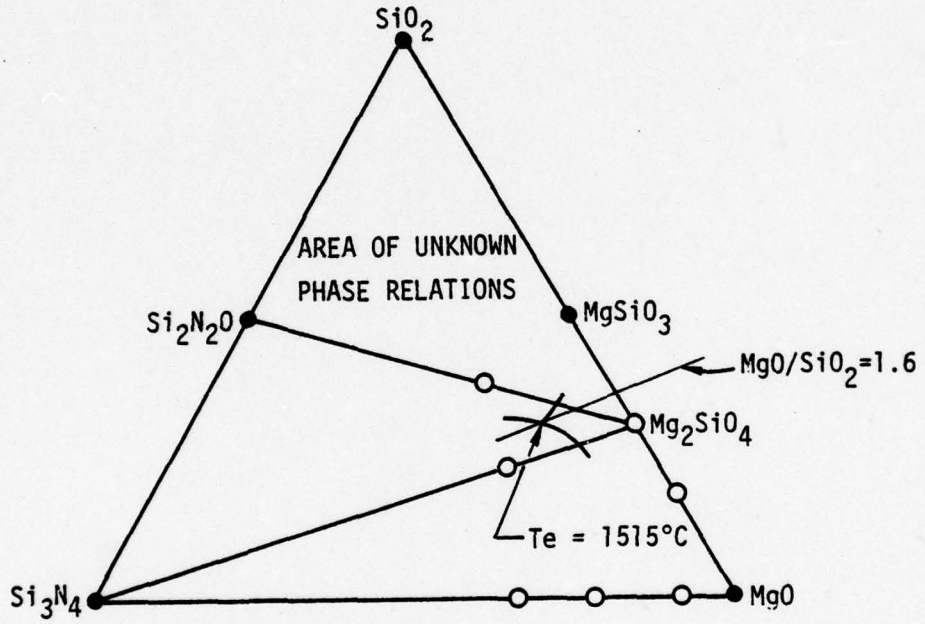
SiO2
AREA OF UNKNOWN
PHASE RELATIONS
Si2N2O
MgSiO3
MgO/SiO2=1.6
Mg2SiO4
Te = 1515°C
Si3N4
MgO

FIGURE 1

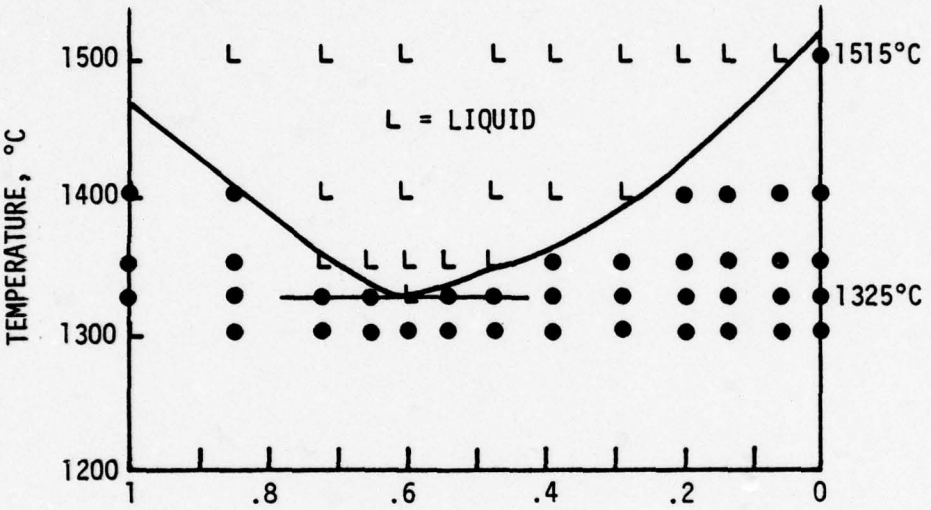
1500
1400
1300
1200
TEMPERATURE, °C
L = LIQUID
1515°C
1325°C
1
.8
.6
.4
.2
0
MOLE FRACTION CaO
IN
0.11 Si_3N_4 + 0.34SiO_2 + 0.55 (MgO, CaO)

FIGURE 2

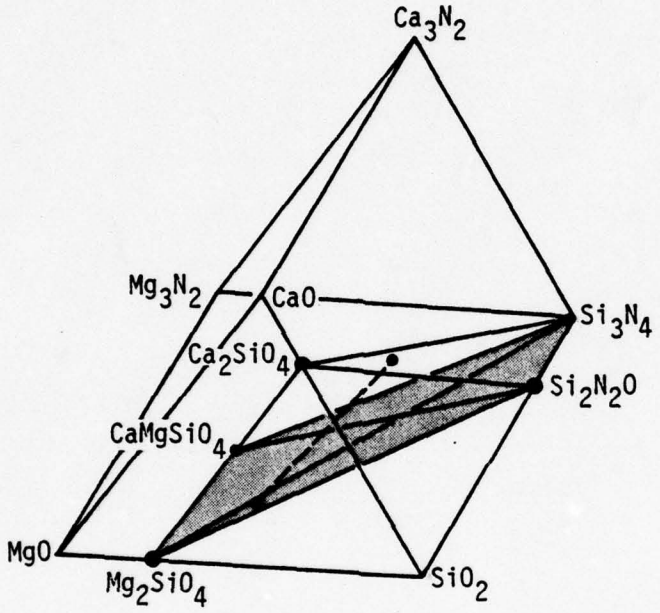
Ca_3N_2
Mg_3N_2
CaO
Si_3N_4
Ca_2SiO_4
Si_2N_2O
$CaMgSiO_4$
MgO
Mg_2SiO_4
SiO_2

FIGURE 3

APPENDIX II

Rockwell International
Science Center
SC5099.1IR

EVIDENCE FOR CAVITATION CRACK GROWTH IN Si_3N_4

F. F. Lange
Structural Ceramics Group
Rockwell International Science Center
Thousand Oaks, California 91360

Above a given temperature, which appears to depend on gross composition[1] and impurities,[2,3], polyphase Si_3N_4 materials exhibits subcritical crack growth.[4,5,6] Since some Si_3N_4 materials are known to contain an amorphous phase,[7,8,9] and recent work has shown that certain compositions fabricated in the Si_3N_4-SiO_2-MgO system containing CaO impurities can have eutectics <1400°C,[10] the formation and linking of cavities in the liquid phase ahead of a crack has been suggested as a mechanism for slow-crack growth.[4,11,12] Observations presented here confirm this mechanism.

Specimens used for a previous study,[1] fabricated with composite powders containing a fixed molar content of Si_3N_4 and different MgO/SiO_2 molar rations were fractured in 4-pt bending at 1400°C in air, cooled to room temperature and subsequently fractured again with a chesile to reveal the microstructure underlying the high temperature fracture surface. Fracture surfaces were examined with a SEM.

The high temperature fracture surface appeared oxidized to different degrees depending on its composition (see Ref. 1). Areas of slow-crack growth similar to those previously reported could easily be identified for

compositions with a $MgO/SiO_2 < 2$. Typically, these areas contained thin wedges of material of different sizes and shapes which were torn away from the main fracture surface, but still firmly attached at one end (see Figures 3 and 4, Ref. 11). That is, the wedges were formed by a large secondary crack which undercut a volume of material. The large crack-opening displacement indicated that a large amount of non-elastic deformation was associated with both the material within the wedge and the secondary crack. Areas of fast crack growth appeared relatively smooth at low magnificatons. At higher magnifications, the topography of both the slow and fast crack growth areas were indistinguishable. As shown in Fig. 1, the topography was formed by the long prismatic Si_3N_4 grains, which appeared to undergo extensive separation from one another, coated with a fluid-like material which could represent the oxidation product produced during fracture at 1400°C. Triple-point voids within the liquid phase were common features. These voids could have been produced by the separation of the grains during fracture and/or subsequent oxidation.

Observations of the room temperature fracture surfaces adjacent to the high temperature fracture surfaces were most revealing. The microstructure beneath the high temperature fracture surface contained many voids and large separations between adjacent grains as shown in Fig. 2. Qualitative observations indicated that the thickness of material containing the large void content increased for materials with compositions closer to the ternary eutectic within the Si_3N_4-Si_2N_2O-Mg_2SiO_4 compatibility triangle[10] (e.g., either by decreasing the Si_3N_4 content, or by shifting toward a MgO/SiO_2 ratio of 1.6). Within a given material, maximum void contents were observed beneath the area of slow-crack growth. It was difficult to discern a

concentrated void phase for materials in which slow-crack growth was not strongly evident (i.e., materials with a MgO/SiO >3). By observing areas at higher magnifications, evidence was obtained for what appeared to have been a viscous phase between grains which had separated during fracture at 1400°C. Figure 3a illustrates the room temperature fracture surface of an apparent viscous phase "pocket" containing a large void. Fig. 3b illustrates "stringers" between two separating grains analogous to the stringers produced by printers ink between two separating plates. Figure 3b illustrates the complete separation of two grains with the remanants of the viscous phase adhering to the separated surfaces. This latter observation was the most frequent of the three. Attempts to etch away the apparent viscous phase with HF were inconclusive because of the difficulty associated with relocating the same area and the presence of etching debris.

In the occasional specimen, the room temperature fracture surface would cut through one of the torn wedges to reveal the microstructure of the material ahead of the secondary crack. As shown by the example in Fig. 4, the secondary crack had propagated by the formation and linking of voids ahead of the crack.

The evidence presented here clearly illustrates that slow-crack growth in polyphase Si_3N_4 occurs by cavitation. Evidence is also presented showing that a liquid can be part of the high temperature microstructure of these polyphase materials and that cavitation appears to initiate within the liquid phase. These observations support an earlier hypothesis that slow-crack growth occurs by accelerated creep[4,11,12] in the high stress field ahead of the crack to produce cavities, which in turn, link together to result in crack extension.

REFERENCES

1. F. F. Lange "Phase Relations in the System Si_3N_4-SiO_2-MgO and Their Interrelation with Strength and Oxidation," J. Amer. Ceram. Soc. 61 (1-2), 53-6 (1978).

2 J. L. Iskoe, F. F. Lange and E. S. Diaz "Effect of Selected Impurities on the High Temperature Mechanical Properties of Hot-Pressed Si_3N_4," J. Mat. Sci 11, 908-12 (1976).

3. D. W. Richerson, Bul. Amer. Ceram. Soc. 52, 560-2 (1973).

4. F. F. Lange "High Temperature Strength Behavior of Hot-Pressed Si_3N_4: Evidence for Subcritical Crack Growth," J. Amer. Ceram. Soc. 57 (2) 84-7 (1974).

5. A. G. Evans and S. M. Widerhorn "Crack-Propagation and Failure Prediction in Si_3N_4 at Elevated Temperatures," J. Mat. Sci. 9, 270 (1974).

6. A. G. Evans, L. R. Russell and D. W. Richerson, "Slow Crack Growth in Ceramic Materials at Elevated Temperatures," Met. Trans. 6A, 707 (A75).

7. A. G. Evans and J. V. Sharp "Microstructural Studies on Si_3N_4," J. Mat. Sci. 6, 1292 (1971).

8. R. Kossowsky "The Microstructure of Hot-Pressed Si_3N_4," J. Mat. Sci. 8, 1603 (1973).

9. D. R. Clarke and G. Thomas "Grain Boundary Phases in a Hot-Pressed MgO Fluxed Si_3N_4," J. Amer. Ceram. Soc. (11-12) 491-95 (1977).

10. F. F. Lange, "Eutectic Studies in the Si_3N_4-Si_2N_2O-Mg_2SiO_4-MgO System" to be published.

11. F. F. Lange, "High-Temperature Strength Behavior of Hot-Pressed Si_3N_4 and SiC; Effect of Impurities," Ceramics for High Performance Applications, Ed. by J. Burke, A. E Gorum, and R. N. Katz, pp. 223-38, Brook Hill (1974).

12. F. F. Lange "Non-Elastic Deformation of Polycrystals with a Liquid Boundary Phase," Deformation of Ceramic Materials, Ed by R. C. Bradt and R. E. Tressler pp. 361-81, Plenum (1975).

ACKNOWLEDGEMENT

This work was supported by the Air Force Office of Scientific Research, Contract No. F49620-77-C-0072.

FIGURE CAPTIONS

Fig. 1 Fracture surface topography produced at 1400°C showing separated, long, prismatic grains of Si_3N_4 coated with an apparent liquid phase.

Fig. 2 Cavitation and grain separation of material underlying 1400°C fracture surface in polyphase Si_3N_4.

Fig. 3 Apparent viscous phase between separating grains of Si_3N_4 (arrows). Observations on room temperature fracture surface within highly cavitated zone underlying 1400°C fracture surface.

Fig. 4 Example of cavitation crack growth in polyphase Si_3N_4.
a) Intersection of room temperature and 1400°C fracture surfaces showing wedge separating from high temperature fracture surface.
b) Higher magnification of secondary crack which produced wedge of material.

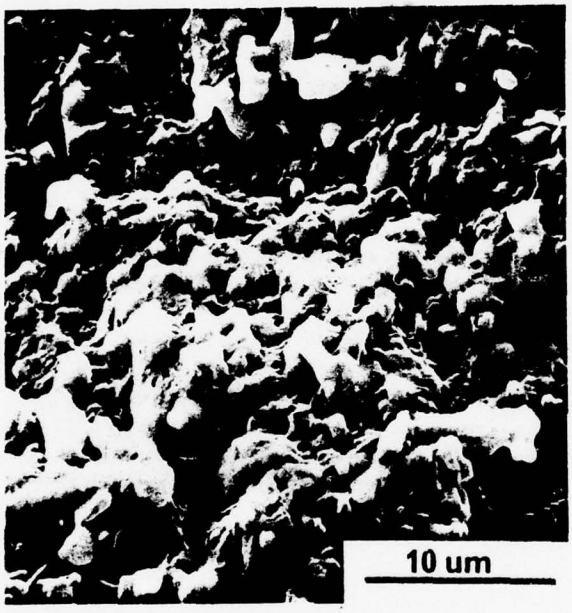

FIGURE 1

FIGURE 2

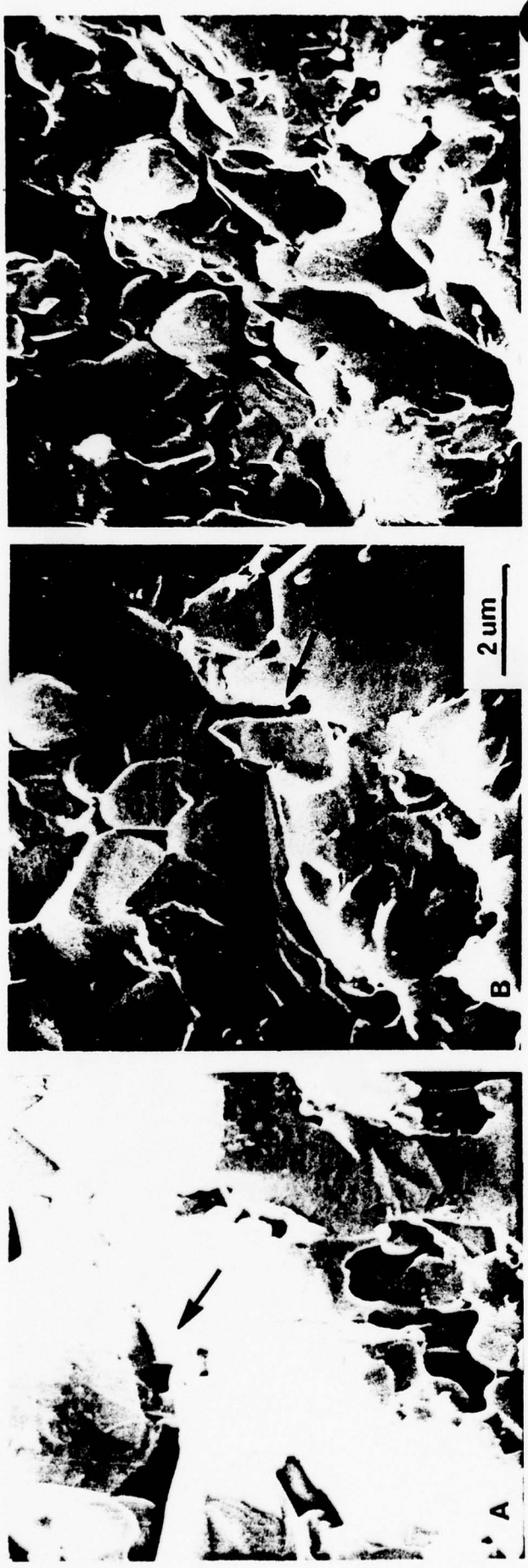

FIGURE 3

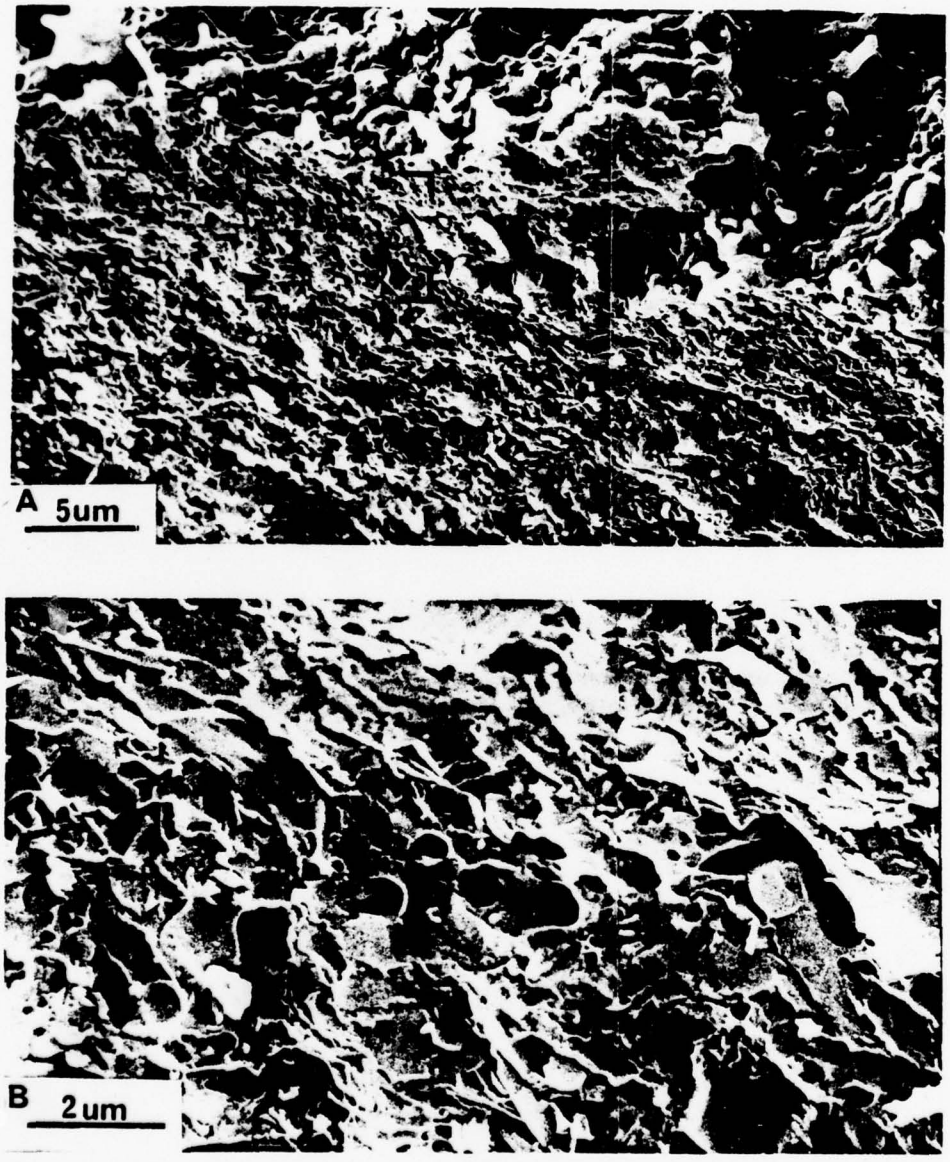

FIGURE 4

APPENDIX III

Rockwell International
Science Center
SC5099.1IR

STRESS INDUCED PENETRATION OF A LIQUID BETWEEN GRAINS BY SOLUTION-REPRECIPITATION

by

F. F. Lange

Rockwell International Science Center
1049 Camino Dos Rios
Thousand Oaks, California 91360

ABSTRACT

The penetration of a viscous liquid, initially located at three grain junctions, to locations between grains is modeled using a solution-reprecipitation mode of material transport and fracture mechanics concepts to derive the chemical potential driving force. Estimates of the time required to completely penetrate grain boundaries in hot-pressed Si_3N_4 are obtained by using diffusion data for the transport of Si in liquid silicates and by relating the diffusion coefficient to viscosity through the Stokes-Einstein relation. Both approaches estimate short penetration periods (< 30 seconds) under moderate stresses for liquid silicates near their melting temperature. For such conditions, the liquid silicates can be considered for all practical purposes (e.g. for modeling creep phenomena) as a thin layer between adjacent grains.

INTRODUCTION

Clarke and Thomas[1] have recently shown through the use of high resolution electron microscopy (viz. lattice fringe imaging) that the amorphous phase in hot-pressed Si_3N_4 is predominantly observed at grain junctions and only occasionally observed as a very thin layer between adjacent grains. Although these observations may not represent the average microstructure at elevated temperatures due to the restrictions concerned with the observation (e.g. the probability of having grain pairs in the proper orientation, etc.) and the fact that a triple point phase may increase its volume fraction by reacting with the grains above the solidus temperature, these observations represent, in the least, location of the amorphous phase when its volume fraction decreases to zero.

The degradation of the high temperature mechanical properties of hot-pressed Si_3N_4 has been qualitatively explained as being caused by a viscous, amorphous phase which allows under an applied stress the separation and sliding of the relatively rigid grains.[2,3,4] Both qualitative and quantitative models used to explain the role of the visous phase assume that it exists as a thin layer between the rigid grains. Most of Clarke and Thomas'[1] observations are contrary to this assumption, and thus a reappraisal of the role of the viscous phase located only at grain junctions appears relevant.

The purpose of this work is to obtain an estimate of the time required for the viscous liquid, assumed only to be located initially at grain junctions, to move between the grains under the action of an applied stress by a solution-reprecipitation phenomenon where it might play a role in the deformation process assumed by current thinking.

MODEL

The high temperature microstructure of the two-phase material, consisting of solid grains with a viscous (e.g. silicate) liquid at triple points is schematically shown in Fig. 1a. This is similar to the majority of the microstructural observations of Clarke and Thomas[1], except their amorphous phase is now assumed to be a viscous liquid. Although the compliance of the composite body is likely to change as the triple-point phase rapidly changes viscosity, the parting of grain centers in the direction of an applied tensile stress, and thus nonelastic deformation phenomena is limited to solid state processes until the liquid completely penetrates between the grains. The questions thus posed are: (a) How can the liquid penetrate between the grains? (b) What is a reasonable period to accomplish this penetration under test conditions?

A reasonable answer to the question of liquid penetration lies with the differential chemical potential of the solid material caused by a magnification of the applied stress at the cusp positions relative to the flatter positions along the solid-liquid interfaces as shown in Figure 1b. The differential chemical potential will cause the solution of material at cusp positions and a reprecipitation at flatter positions to change the shape (but not the volume) of the liquid inclusion such that it penetrates between the grains.

Liquid penetration can be considered as the growth of a liquid-filled crack, where the rate limiting process is assumed to be the diffusion of the dissolved solid at the crack front through the liquid to positions of lower chemical potential. Using this approach, the change in the stress intensity, and thus the chemical potential, at the cusp position with increasing penetration can be handled using fracture mechanics concepts.

As shown in Fig. 1c, the crack front, defined by a radius of curvature of molecular dimensions, can advance by dc when an incremental volume

$$dV \simeq 2\rho z dc = V_o dn. \tag{1}$$

is dissolved and transported to surfaces away from the crack front by the molecular flux

$$J = \frac{1}{2\rho z} \frac{dn}{dt} . \tag{2}$$

V_o is the molecular volume and dn is the incremental number of molecules transported. Thus, the velocity of liquid penetration is

$$\frac{dc}{dt} = -V_o J. \tag{3}$$

Following Stocker and Ashby[5], the molecular flux is related to the chemical potential gradient $\nabla\mu$ by

$$J = - \frac{D_L C_L}{V_o kT} \nabla\mu, \tag{4}$$

where D_L = diffusion coefficient of the dissolved species in the liquid, C_L is the dimensionless molecular fraction of the dissolved material in the liquid and kT has the usual meaning.

The chemical potential gradient $\nabla\mu = \frac{\Delta\mu}{\Delta x}$ is assumed to be constant along the length of the crack, i.e. $\Delta x = c$. The differential chemical potential $\Delta\mu$ is

$$\Delta\mu = \mu - \mu_o = kT \frac{a}{a_o} = \Delta\sigma V_o, \tag{5}$$

where a and a_o are the activities of the solid at the crack front and at the remote liquid-solid surfaces, respectively. The differential stress $\Delta\sigma = \sigma_m - \sigma_o$, where σ_m is defined by the Inglis[6] relation

$$\sigma_m = 2\sigma_a \left(\frac{c}{\rho}\right)^{1/2} \tag{6}$$

and σ_o is the stress at the remote liquid-solid surfaces. Since $\sigma_m >> \sigma_o$,

$$\Delta\sigma = \sigma_m = 2\sigma_a \left(\frac{c}{\rho}\right)^{1/2}. \tag{7}$$

Combining these relations,

$$J = - \frac{2D_L C_L \sigma_a}{kT \rho^{1/2}} \; c^{-1/2}, \tag{8}$$

and thus, the rate of liquid penetration is

$$\frac{dc}{dt} = \frac{2V_o D_L C_L \sigma_a}{kT\rho^{1/2}} \; c^{-1/2}. \tag{9}$$

The time, t_p, for the liquid to completely penetrate the grain boundary (i.e. a distance of G/2) can be determined by integrating equation (9):

$$t_p = \frac{kT\rho^{1/2}}{3V_o D_L C_L \sigma_a} \left[(G/2)^{3/2} - (c_o)^{3/2}\right] \tag{10}$$

Since G is usually > c_o,

$$t_p \approx \frac{kT_o^{1/2}}{3V_o D_L C_L \sigma_a} \quad (G/2)^{3/2} \qquad (11)$$

ESTIMATING PENETRATION TIME FOR POLYPHASE Si_3N_4

Penetration times can be estimated for polyphase Si_3N_4 by substituting into equation (11) reasonable values for the various factors. Factors known without much ambiguity are the molecular volume of Si_3N_4 ($V_o = 7.3 \times 10^{-29}$ m^3/molecule) and the average grain size ($G = 10^{-6}$ m). Recent work by the author has shown that the ternary eutectic compositions close to the Si_3N_4-Mg_2SiO_4 tie line contain ~ 0.1 mole fraction of Si_3N_4, suggesting a reasonable value of $C_L = 0.1$. Values of crack front radius can be estimated from the lattice fringe imaging micrographs published by Clarke and Thomas[1], suggesting a value of $\rho \approx 10^{-9}$ m.

Two approaches can be used to estimate the coefficient of diffusion, D_L. First, it can be assumed that the liquid is a complex silicate containing much of the impurities as indicated by Auger analysis[7,8] and that the diffusivity is governed by the mobility of the slowest moving ion or radical. Second, it can be assumed that the diffusivity is determined by the Stokes-Einstein equation which relates the coefficient of diffusion to the viscosity of the liquid. Both of these approaches will be discussed to estimate t_p.

In the first approach, the coefficient of diffusion for the slowest moving ion is sought. As indicated in Frischat's[9] recent review of diffusion in glasses, relative to other common constituents, Si (or $(SiO_4)^{-4}$ radicals) has the lowest mobility, both above and below the glass transition temperature. Diffusivity data for Si is limited to measurements on a calcium-aluminum-silicate slag which has similarities to the Ca-Mg-Al silicate glass compositions believed to be present in polyphase Si_3N_4[7,8]. These measurements[10] indicate a coefficient of diffusivity for Si of 10^{-12} to 10^{-11} m^2/sec at temperatures between 1350°C and 1450°C. Choosing T = 1623°K (1350°C), $D = 10^{-12}$ m^2/sec and σ_a = 70 MPa

(10,000 psi), $t_p \approx 1$ sec.

In the second approach, the Stokes-Einstein relation[5]

$$D_L = \frac{kT}{8\eta V_o^{1/3}} \tag{12}$$

is substituted into equation (11); η=viscosity. Doremus[11] has discussed the limitations of using the Stokes-Einstein relation in predicting diffusivity, but he indicates its approximate validity for predicting the mobility of Si in silicates. Stocker & Ashby[5] are more adamant in the general use of the Stokes-Einstein relation for predicting D_L. Thus, substituting equation (12) into equation (11) one obtains

$$t_p = \frac{8\eta\rho^{1/2}}{3V_o^{2/3} C_L \sigma_a} (G/2)^{3/2} . \tag{13}$$

The results of equation (13) are illustrated in Figure 2 which plots penetration time vs viscosity for an applied stress of 35, 70 and 150 MPa and values for the other factors given above. This figure shows that complete penetration of the viscous silicate between the grains can occur in relatively short periods under moderate stresses, viz. ~ one hour for a viscosity of $\sim 10^6$ poise and < 30 sec. for viscosities in the melting range. This latter condition is in agreement with the first approach to estimate t_p using known diffusion coefficients for Si in a molten silicate glass.

These penetration times can be considered as upper bound estimates for two reasons. First, a linear chemical potential function has been assumed; penetration times would be much less if, for example, a parabolic function was assumed. Second, the calculation neglects the stress field interaction of the

opposing liquid-filled cracks, that eventually meet near the center of the grain boundary. The interacting stress fields would increase the value of σ_m from that assumed in Eq. (6) and therefore decrease the penetration time. Thus, penetration times obtained by either Eqns. (11) or (12) can be considered as upper bound estimates.

In conclusion, it has been shown that if the glassy phase within a ceramic is only located at grain junctions, the viscous glass can penetrate between the grains by a solution-reprecipitation process. Estimates for the period in which the viscous liquid can completely penetrate can be obtained using either equation (11) when the diffusion coefficient of the slowest moving species is known or equation (13) when the viscosity is known. It has been estimated that when the glassy silicate approaches its melting temperature, the penetration period under relatively low stresses is of the order of several seconds for materials with a grain size ~ 1 μm. For this condition, it is reasonable to chose deformation models in which the microstructure consists of rigid grains separated by a fluid. Such models may invoke liquid diffusivity of the Nabarro-Herring type [5] and/or fluid flow/cavitation phenomena [3] to explain the deformation kinetics. On the other hand, when either the liquid diffusivity is low, e.g. $< 10^{-16}$ m^2/sec or the viscosity is high, e.g. $> 10^7$ poises, penetration periods will be > 10 hrs. and models invoking solid state processes (e.g. volume and/or grain boundary diffusion) must be used to explain, at least, early stage deformation phenomena.

ACKNOWLEDGMENTS

Helpful discussions with A. G. Evans were greatly appreciated. This work was supported by the Air Force Office of Scientific Research, Contract Number F44620-77-C-0072.

REFERENCES

1. D. R. Clarke and G. Thomas, "Grain Boundary Phases in a Hot-Pressed MgO Si_3N_4", J. Amer. Ceram. Soc. (in press).
2. F. F. Lange "High-Temperature Strength Behavior of Hot-Pressed Si_3N_4: Evidence for Subcritical Crack Growth", J. Amer. Ceram. Soc. 57, 84 (1974).
3. F. F. Lange, "Non-Elastic Deformation of Polycrystals with a Liquid Boundary Phase", Deformation of Ceramic Materials, Ed. by R. C. Bradt and R. E. Tressler, pp 361-381, Plenum (1975).
4. R. Kossowsky, D. G. Miller, E. S. Diaz, "Tensile and Creep Strengths of Hot-Pressed Si_3N_4", J. Mat. Sci. 10, 983 (1975).
5. R. L. Stocker and M. F. Ashby, "On the Rheology of the Upper Mantle", Rev. Geophysics and Space Phys. 11, 391 (1973).
6. C. E. Inglis, "Stresses in a Plate due to the Presence of Cracks and Sharp Corners", Proc. Inst. Naval Architects 60, 219 (1913).
7. R. Kossowsky, "The Microstructure of Hot-Pressed Si_3N_4", J. Mat. Sci. 8, 1603 (1973).
8. B. D. Powell and P. Drew, "Identification of a Grain Boundary Phase in Si_3N_4", J. Mat. Sci. 9, 1867 (1974).
9. G. H. Frischat, Ionic Diffusion in Oxide Glasses, Trans. Tech. Publications, Germany (1975).
10. H. Towers and J. Chipman, Trans. Amer. Inst. Min. Engrs. 197, 1455 (1953).
11. R. H. Doremus, "Diffusion in Non-Crystalline Silicates", pp 1-71, Modern Aspects of the Vitreous State 2, Ed. by J. D. MacKenzie, Butterworths (1962).

FIGURE CAPTIONS

Figure 1 Schematic of polycrystalline microstructure containing a viscous liquid at grain junctions.

Figure 2 Time (t_p) for liquid to completely penetrate between grains versus viscosity of liquid silicate.

SC5099.1IR

a

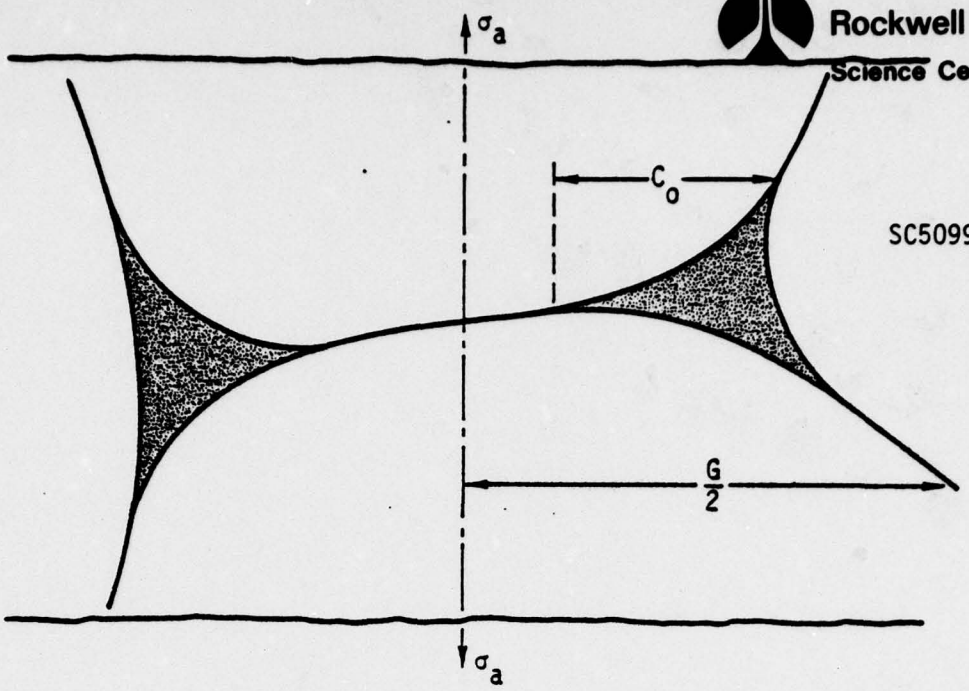

b

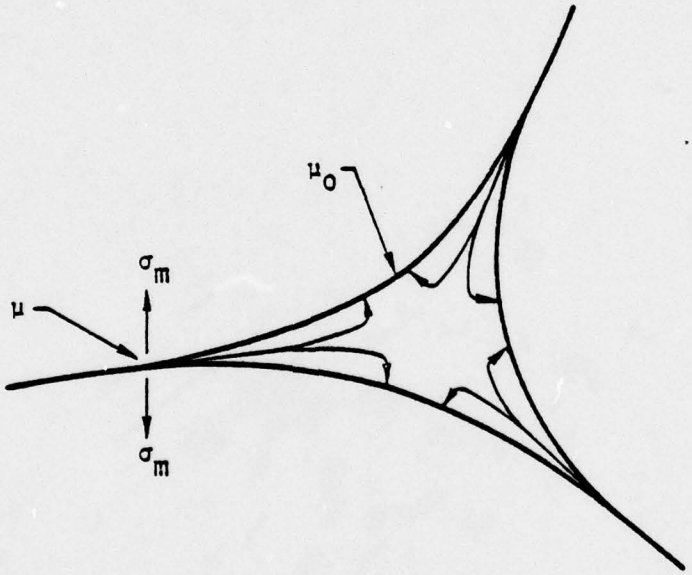

c

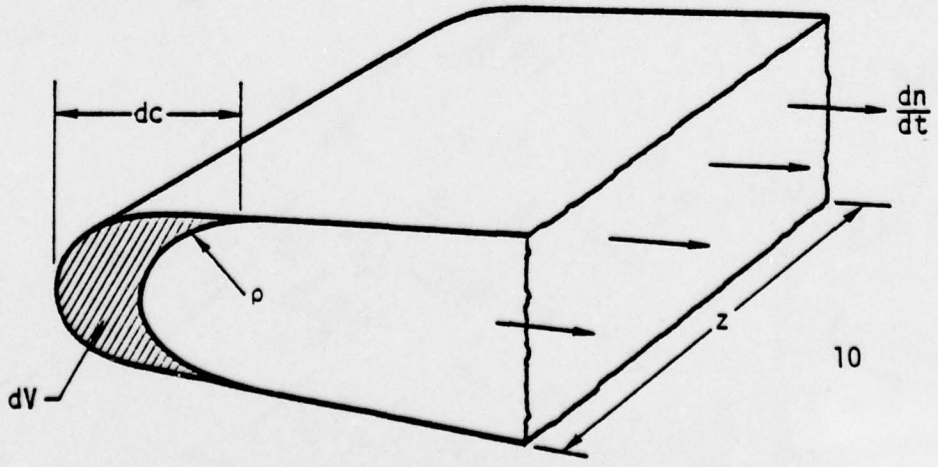

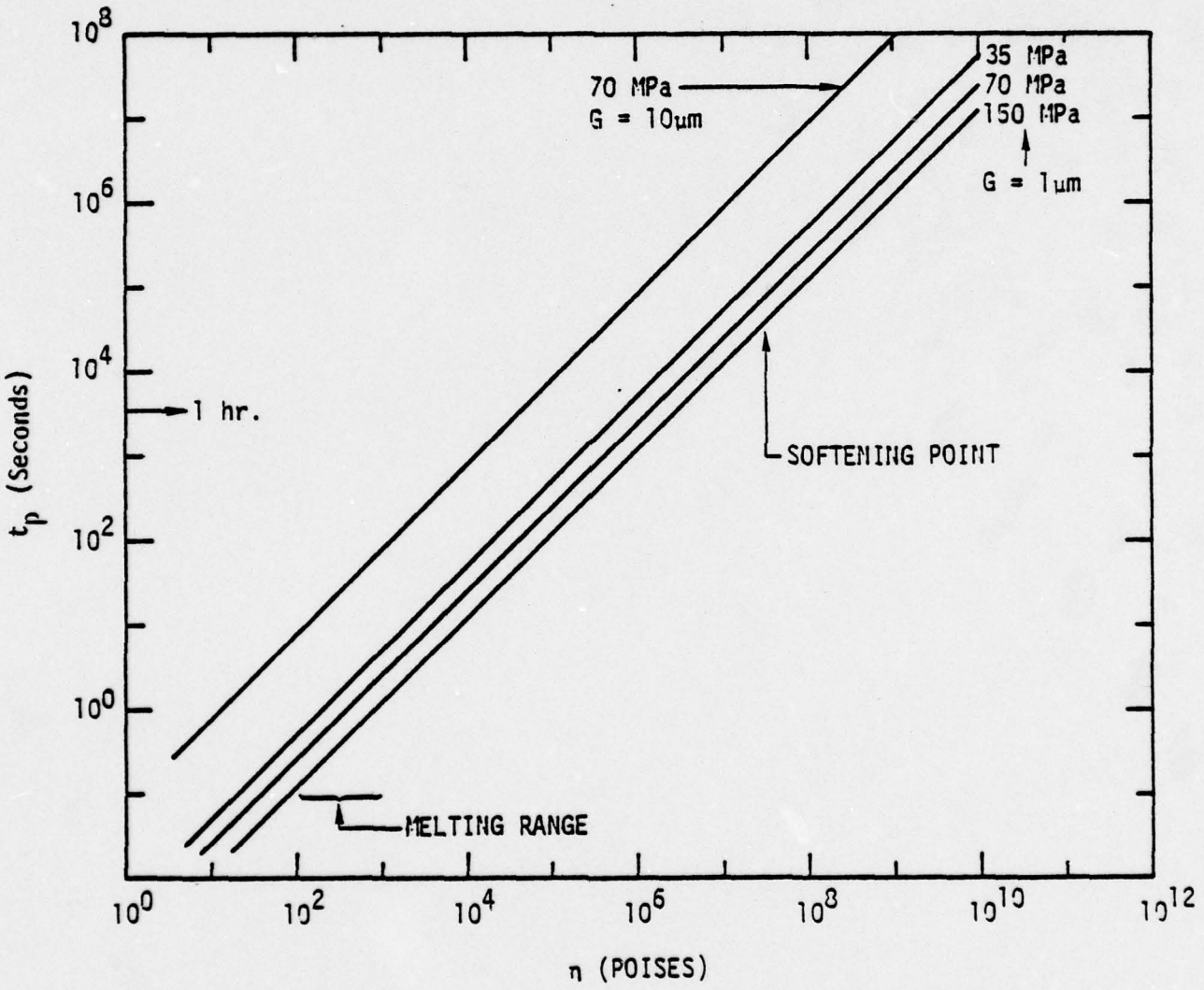
10^8
10^6
10^4
10^2
10^0
t_p (Seconds)
1 hr.
70 MPa
G = 10μm
35 MPa
70 MPa
150 MPa
G = 1μm
SOFTENING POINT
MELTING RANGE
10^0
10^2
10^4
10^6
10^8
10^{10}
10^{12}
η (POISES)

APPENDIX IV

REACTION OF IRON WITH Si_3N_4 MATERIALS TO PRODUCE SURFACE PITTING

F. F. Lange

SC5099.1IR

Structural Ceramics Group
Rockwell International Science Center

The purpose of this note is to show that surface pits result from the reaction of Fe with most Si_3N_4 alloys fabricated with MgO, whereas pitting does not result for certain Si_3N_4 alloys fabricated with Y_2O_3.

Singhal[1] has shown that the long term oxidation of commercial Si_3N_4 fabricated with MgO leads to degradation of flexural strength ranging from 30% for periods $\geq$ 300 hrs. at 1100°C to 60% for $\geq$ 100 hrs at 1375°C. Large surface pits formed during oxidation appear responsible for the degradation, e.g. pits are common fracture origins and strength can be regained after removing the pits by surface grinding.[1] Similar, but less extensive oxidation/strength testing of Si_3N_4 fabricated within the Si_3N_4-Si_2N_2O-$Y_2Si_2O_7$ system only leads to $\sim$ 15% strength reduction for oxidation periods up to 400 hrs. at 1375°C[2]; surface pitting was not observed for this material.

The formation of surface pits during oxidation suggests the presence of heterogeneously distributed reactive sites. Sources for such sites could include aggregated second phases, large contaminate particles introduced during fabrication, and furnace debris. Although aggregated second phase particles are likely sources for Si_3N_4 hot-pressed with MgO*, the effect of large contaminate particles was sought in the present work.

* As detailed elsewhere[3], the magnesium compounds present in Si_3N_4-MgO alloys are not compatible with SiO_2, the oxidation product of Si_3N_4.

A number of large, metallic appearing particles were located on the surface of commercial NC132 Si_3N_4 with light microscopy. As shown in Fig. 1, the particles were typically aggregated; aggregated sub-surface particles could be observed with crossed polars. Each group of particles were relocated in a SEM and identified with the aid of EDAX. All particles consisted of Si, W and Fe; a few also contained Ni, Cr and/or Co. Others[4,5] have reported observing similar contaminates in hot-pressed Si_3N_4. WSi_2 is a common contaminate due to the WC media used to mill the powder prior to hot-pressing. Fe is a common contaminate; it is added by some workers[6] to increase the nitriding rate in producing Si_3N_4 powder.

Short period oxidation tests at 1300°C and 1400°C indicated greater reactivity at the impurity sites which could be relocated, but due to the ambiguity of relocating most of the sites beneath the oxide scale, a second group of experiments were conducted. In the new experiments, small particles ($\sim$ 200μm) of Fe were placed on the surfaces of different Si_3N_4 materials. Emphasis was placed on Fe due to the volatile nature of tungsten oxides. The Si_3N_4 materials investigated included NC132 Si_3N_4*, a series of materials containing 0.83 mole fraction Si_3N_4 with different MgO/SiO_2 molar ratios (see ref. 3), and Si_3N_4 fabricated with 0.840, 0.055, and 0.105 mole fraction of Si_3N_4, Y_2O_3 and SiO_2, respectively (see ref. 7). Each specimen was oxidized at 1400°C for periods up to 4 hrs.

For the series of materials with different MgO/SiO_2 molar ratios, the surface reaction at the site of the Fe particle ranged from no apparent reaction for the material with a MgO/SiO_2=0.1, to a glassly reactive zone containing a shallow pit for $0.1 < MgO/SiO_2 < 0.5$, to a highly reactive, deeply pitted area for $MgO/SiO_2 < 0.5$ as illustrated in Fig. 2. The reactive area for NC132 Si_3N_4

* Norton Co., Worchester, Mass.

was similar to the material within the series with a MgO/SiO_2 = 0.5. Surface cracks, presumed to form during cooling, were observed within all reactive zones. As shown in Fig. 3, no apparent reaction occurred for the $Si_3N_4/Y_2O_3/SiO_2$ material.

These results show that surface pitting produced during the oxidation of Si_3N_4-MgO alloys can be caused by heterogeneously distributed Fe contaminates and that the reactivity/pitting increases as the MgO/SiO_2 molar ratio is increased. Previous studies[3] have shown that when $MgO/SiO_2 > 2$, the equilibrium secondary phases are Si_2N_2O and Mg_2SiO_4 and when $MgO/SiO_2 < 2$, the secondary phases are Mg_2SiO_4 and MgO. Non-equilibrium magnesium-silicate-nitrogen glasses are presumed to be present also. The reaction in oxidizing environments between Fe and the secondary phases is presumed to involve FeO and SiO_2, the oxidation products of Fe and Si_3N_4, respectively, and the equilibrium/non-equilibrium magnesium phases present in Si_3N_4-MgO alloys. Such reactions can produce relatively low temperature eutectics.[8] The absence of significant reactivity in the $Si_3N_4/Y_2O_3/SiO_2$ material indicates a tolerance for Fe contamination in this system without severe oxidation/strength degradation.

ACKNOWLEDGEMENT

This work was supported by the Air Force Office of Scientific Research, Contract No. F49620-77-C-0072.

REFERENCES

1. S. C. Singhal "Strength Degradation of Si_3N_4 Due to Oxidation", to be published; A. F. McLean, E. A. Fisher, R. J. Bratton and R. J. Miller, "Brittle Materials Design, High Temperature Gas Turbine", Interim Reports. AMMRC-CTR-75-28, Sept. 1975 and AMMRC-CTR-76-12, April 1976.

2. F. F. Lange and S. C. Singhal, unpublished work.

3. F. F. Lange "Phase Relations in the Si_3N_4-SiO_2-MgO Systems and Their Interrelation with Strength and Oxidation", J. Amer. Ceram. Soc. (in press).

4. R. Kossowsky, "The Microstructure of Hot-Pressed Si_3N_4", J. Mat. Sci. 8, 1603 (1973).

5. H. R. Baumgartner and D. W. Richerson "Inclusion Effects on the Strength of Hot-Pressed Si_3N_4", Fracture Mechanics of Ceramics, Vol. 1, p. 367, ed. by R. C. Bradt, D. P. H. Hasselman and F. F. Lange, Plenum Press, New York 1974.

6. P. Popper and S. N. Ruddlesden, "Preparation, Properties and Structure of Si_3N_4", Trans. Br. Ceram. Soc. 60 (9) 603-26 (1961).

7. F. F. Lange, S. C. Singhal and R. C. Kuznicki, "Phase Relations and Stability Studies in the Si_3N_4-SiO_2-Y_2O_3 Psendo-Tesnary System", J. Amer. Ceram. Soc. 60 (5-6), 249 (1977)

8. E. M. Levin and H. F. McMurdle, Phase Diagrams for Ceramists: 1975 Supplement The American Ceramic Society, Inc. (1975).

FIGURE CAPTIONS

Fig. 1 SEM micrograph of ground and partially polished surface of NC132 Si_3N_4 illustrating aggregated inclusions consisting of Si, W and Fe.

Fig. 2 SEM micrograph of surface pit and reactive zone formed during the oxidation (1400°C/1/2h) of a Fe particle on hot-pressed Si_3N_4 with a composition containing 0.83 mole fraction Si_3N_4 and a MgO/SiO_2 molar ratio of 5.

Fig. 3 SEM micrograph illustrating relatively little reaction between Fe particle and $Si_3N_4/Y_2O_3/SiO_2$ material after oxidation at 1400°C/4 hr. Part of iron oxide particle has been removed to illustrate reactive surface.

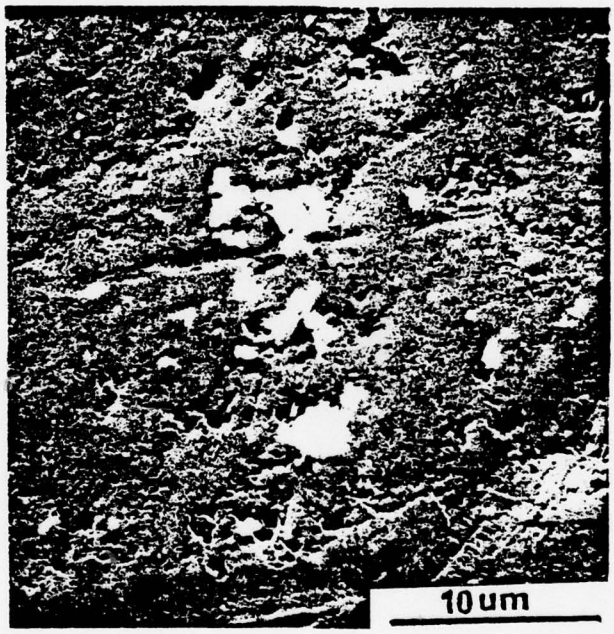

Figure 1

F. F. Lange

Fig 1

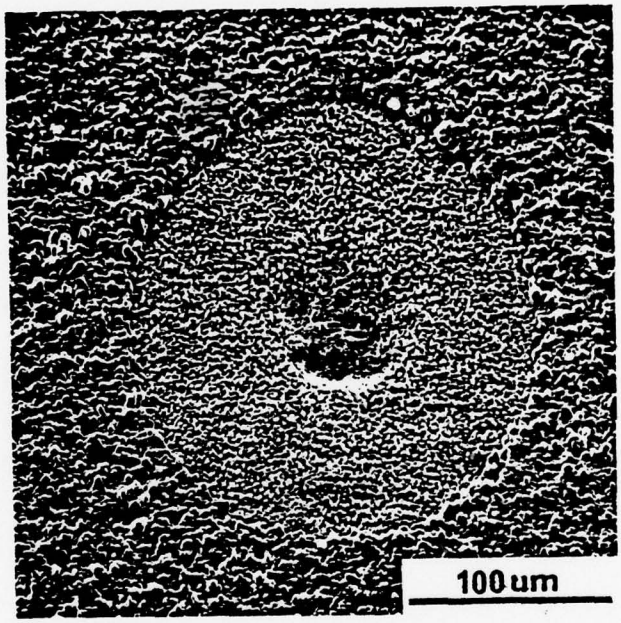

Figure 2

F. F. Lange

Fig 2

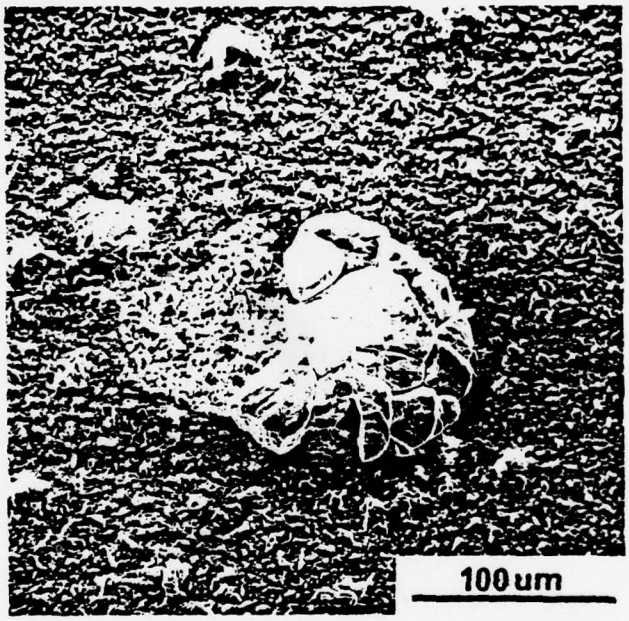

Figure 3

E. F. Louse

Fig 3

APPENDIX V

Rockwell International
Science Center
SC5099.1IR

DENSE SILICON NITRIDE CERAMICS: FABRICATION AND INTERRELATIONS WITH PROPERTIES

F. F. Lange

Rockwell International Science Center

Thousand Oaks, California 91360

1. INTRODUCTION: GENERAL TECHNOLOGY

Powder routes are used to fabricate dense Si_3N_4. Efforts to sinter pure Si_3N_4 powder have not been successful[1], presumably due to insufficient volume diffusivity, decomposition at temperatures $\geq 1850^oC$[2] and volatilization caused by active oxidation[3] in the low oxygen partial pressures required to prevent the formation of SiO_2. Deeley et al.[4] discovered that Si_3N_4 could be fabricated by hot-pressing powders containing a densification aid. Today, many metal oxides and some nitrides are known densification aids. Although hot-pressing currently results in a superior product, the feasibility of pressureless sintering with a densification aid has been demonstrated[5-8].

Densification of Si_3N_4 powder with the aid of a metal oxide is generally attributed to the presence of a liquid formed at high temperatures according to the general reaction:

$$Si_3N_4 + SiO_2 + \text{metal oxide} + \text{impurities} \rightarrow Si_3N_4 + \text{Liquid} \quad (1)$$

where SiO_2 is present either as a surface layer on each particle or as Si_2N_2O. Neglecting possible mass losses caused by volatilization, the composition of the liquid and equilibrium fraction of solid Si_3N_4 will depend on the composition of the starting powder, the phase equilibria of the composite system, and the densification temperature. The apparent role of the liquid is

to promote mass transport by the solution-reprecipitation of Si_3N_4, which results in the disappearance of the voids and thus, densification.

Upon cooling, the liquid solidifies: Si_3N_4 + Liquid → Si_3N_4 + secondary phases. The number, chemistry and content of the secondary phases depend on the composition of the starting powder, and the phase relations in the composite system. Non-equilibrium phases, e.g. glassy silicates, are observed.[9-12] In addition, the crystal structure of Si_3N_4 can be expanded or contracted by the concurrent substitution of certain metal cations for silicon and oxygen for nitrogen.[13] As expected, the secondary phases and the solid-solution alloying of Si_3N_4 can significantly influence all properties. [14,15,16]

The present day manufacture of dense Si_3N_4 can be divided into three steps: 1) manufacture of Si_3N_4 powder by reacting silicon with nitrogen, 2) preparation of powder for densification by adding the required densification aid and reducing the particle size by milling, and 3) densification of the composite powders by either hot-pressing or sintering. The exact mechanics of each step have been developed through individual experience; commerical practice is proprietary. The principal objective here will be to show the known and/or hypothetical interralation between these three steps through the development of microstructure and properties.

2. POWDERS

2.1 Silicon: The Raw Material

Silicon, the second most abundant terrestial element, is commercially produced in carbon-electrod furnaces by a thermochemical reaction between crushed quartzite rock and high purity coke. Excess SiO_2 prevents the formation of SiC. The molten Si is tapped, cast cooled and pulverized to produce a crude powder that is ~98% pure. Acid washing can increase the purity to ~99.5%. Further purification requires the synthesis of a volatile silicon compound. Needless to say, as indicated by chemical analysis, most current producers of Si_3N_4 start with acid washed,'crude' silicon.

The major cation impurities in 'crude' silicon are Fe, Al, Ca and Mg which reflect the major impurities in the raw materials and the iron implements used for pulverizing. Oxygen is the major impurity in silicon powder. Of the major impurity cations listed above, only Al does not form a silicide. It can be presumed that the major impurities can be present as silicides, oxides or complex silicates.

2.2 Si_3N_4: The Starting Powder

Although Si_3N_4 powder can be produced by vapor phase reaction using volatile silicon compounds, only the current, commercial process of reacting silicon powder with nitrogen will be discussed.

It is obvious that the oxygen partial pressure in the nitriding environment should be less than that required to form SiO_2. A less obvious corrolary is that the proper nitriding environment defines the conditions of active oxidation[13], i.e. the formation of volatile SiO. As seen below, SiO appears to play an important role in the nitriding process.

Experience has shown that the reaction of nitrogen with pure, semiconductor grade silicon does not go to completion, viz, very little Si_3N_4 is formed over reasonable reaction periods. The work of Atkinson et al.[18] has shown that Si_3N_4 nuclei first form on the pure silicon surface. As summarized in Fig. 1, these nuclei grow across the surface by a vapor phase reaction which is evident by the concurrent growth of surface pits between the nuclei. Reaction is prematurally terminated when the growing nuclei impinging on one another closing the Si surface from further reaction. Atkinson et al.[18] suggest that Si is the volatile species, but Lange[19] pointed out that SiO vapor is more probable. The proposed cyclic reaction, which involves the active oxidation of Si, the reaction of SiO with N_2 to form Si_3N_4 with the concurrent release of oxygen is shown in Fig. 1.

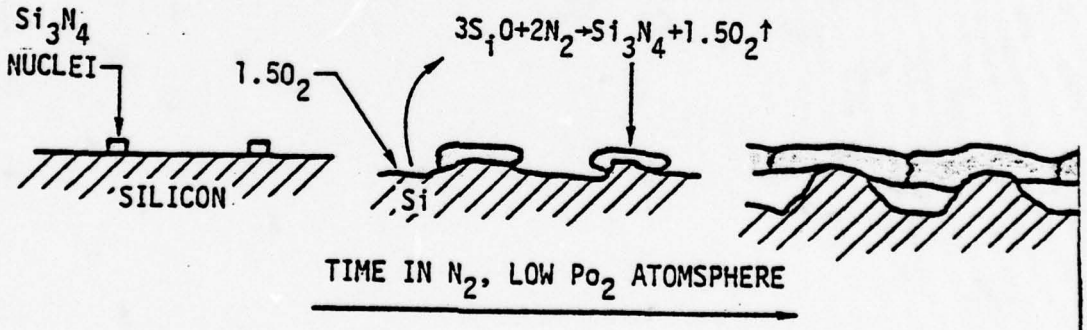

FIGURE 1

Reaction kinetics are greately enhanced when one of a number of different metal nitriding aids are added to semiconductor grade silicon.[20-22] High reaction kinetics are also observed for acid-washed 'crude' silicon which contains the desired contaminant. The role of the nitriding aid is still uncertain, but several rules are apparent. First, the nitride of the metal additive must have a higher free energy of formation than Si_3N_4. For example, the formation of Mg_3N_2 and ALN is more favorable than Si_3N_4 and neither Mg nor Al are nitriding aids; conversly, both Fe and Mn are good nitriding aids. Second, the nitriding aid is only effective above the metal-Si eutectic temperature. These rules suggest that particles of the metal nitriding aid reacts with the surrounding silicon particles to form a silicon-rich liquid in equilibrium with the remaining silicon. The active oxidation of the metal-silicon liquid produces volatile SiO which reacts with N_2 to form Si_3N_4. As active oxidation depletes the metal-Si liquid of silicon, the liquid further dissolves the surrounding silicon to maintain an equilibrium composition. In this manner, the metal-Si liquid 'eats' its way through the surrounding silicon unhampered by surface closure, producing volatile SiO to form Si_3N_4 by a vapor phase reaction.

Most Si_3N_4 powders produced by nitriding contain the two hexagonal crystal structures, α- and β-Si_3N_4. Since either structure can be produced from the other by a 180^0 rotation of two Si containing stacking planes (viz. β (abab...)→α (abcd... = abqe ...)), the transformation requires reconstruction (e.g. through solution and reprecipitation). Although both structures are well known[23-26], their thermodynamic interrelation is still in question. This is a critical question since high α-phase powders are required to produce the tough, strong material.[27] Experience suggests that nitriding temperatures $<1325^0$C result in high α/β ratios. Since the reaction is exothermic, the volume of the material is important for temperature control.[28] Other factors also appear important. Most investigators agree that α-Si_3N_4 forms through vapor phase reactions.

The oxygen content (the major impurity in most powders, with the possible exception of unreacted silicon) is controlled by the nitriding environment (furnaces with porous refractories usually result in high oxygen contents). Oxygen contents have been observed to range between 0.4 to 4.0 wt%.[29] If it is assumed that the oxygen is in the form of SiO_2, this range converts to 2-14 mole% SiO_2. That is, SiO_2 is a powder constituent that cannot be neglected.

2.3 Powder Preparation

The cake of Si_3N_4 formed by nitriding must be reduced to powder by pulverizing and milling. The metal oxide(nitride) densification aid(s) are usually mixed with the Si_3N_4 powder by liquid milling with tungsten carbide milling media. Polymer mill jars help to eliminate contaminanants other than carbon. Silicon nitride can be hydrolyzed to some extent by the liquid milling agent, e.g. Si_3N_4 milled in water produces strong ammonia odors. Dry alcohols reduce this tendency.

The dried, milled powder can be air-classified to minimize the number of large, un-milledagglomerates and much of the dense tungsten arbide contamination. Large contaminate particles or Si_3N_4 agglomerates left in the composite powders can be carried through to the dense material and act as flaws to increase the observed scatter in strength values.[30]

3. PHASE RELATIONS

3.1 Densification Procedures

The composite powders are usually hot-pressed in graphite dies at temperatures between 1650°C and 1750°C for several hours under 28 MPa (4000psi) pressure. Boron nitride slurries are used to coat the graphite parts to ease material removal. Liners made of graphite paper are more desirable for this purpose since the BN becomes embedded in the surface of the hot-pressed billet. Cold-pressing the composite powder in steel dies prior to placing them in the graphite dies eliminates the possibility of contamination with loose graphite particles.

Pre-pressed powder shapes to be pressureless-sintered are embedded within either Si_3N_4 powder or loose powder of the same composition.[3,6] This technique minimizes weight losses due to volatilization to values ≤ 2 wt%. At temperatures <1800°C, volatilization appears to be caused by active oxidation.[3] Thus, techniques which minimize the availability of oxygen to the powder are required to minimize compositional changes and to maximize the sintering phenomena.

3.2 Densification Kinetics and the $\alpha \rightarrow \beta$ Conversion

Densification kinetics of Si_3N_4 powder hot-pressed with the aid of ~15 mole% MgO (~5 wt%) has been obtained by Terwilliger and Lange,[31] and Brook et al.[32]. Terwilliger and Lange obtained apparent activation energies in the range of 700 kJ $mole^{-1}$ (1500°C to 1700°C) and illustrated that the densification kinetics of both high α and high β powders are

similar for comparable powder processing. Brook et al. reports activation energies of 700 kJ $mole^{-1}$ at temperatures $<1550^{o}C$ and 450 kJ $mole^{-1}$ at temperatures $>1550^{o}C$. They suggested that liquid phase sintering occurs in the higher temperatures regime. Both groups show that the densification kinetics increases linearly with applied pressure (7 to 35 MPa) and with the MgO content (3 to 28 mole% MgO). Neither group investigated the effect of SiO_2 (e.g. in terms of the MgO/SiO_2 molar ratio) on the densification kinetics. Adequate correlations have not been made between densification kinetics and the content of the liquid phase responsible for densification.

The $\alpha \rightarrow \beta$ conversion is concurrent with densification. Brook et al.[32] obtained the same activation energies for the conversion as they obtained for densification, strongly suggesting that the mechanisms responsible for mass transport are the same for both phenomena. Both Iskoe and Lange[33] and Brook et al. have shown that the $\alpha \rightarrow \beta$ conversion occurs at a slower rate relative to densification, i.e. full densification can be achieved prior to full $\alpha \rightarrow \beta$ conversion. Full densification only requires the mass transport of a portion of the initial powder, therefore much of the $\alpha \rightarrow \beta$ conversion should take place after densification.

Lange[27] was the first to recognize that an equiaxed grain morphology was obtained with high β starting powders and a fibrous grain morphology resulted from a high α starting powder. The fibrous microstructure results in a higher fracture toughness and strength relative to the equiaxed microstructure[27]. Thus, high α-Si_3N_4 starting powders are required to obtain optimum mechanical properties. Iskoe and Lange[33] observed that the growth of a fibrous microstructure is concurrent with the $\alpha \rightarrow \beta$ conversion. Based on these observations and the assumption that grain growth perpendicular to the fiber axis (c-axis) could be neglected, it was shown[32] that the aspect ratio (R) of the fibers would depend on the initial α/β ratio:

$$R = 1 + \alpha/\beta. \qquad (2)$$

This relation was obtained by assuming that the growth of the grains occurred by the preferential solution of the α particles and reprecipitaion of Si_3N_4 on pre-existing β particles. In addition, the distribution of fiber diameter should be the same as the initial particle size distribution. This model suggests that both the fiber diameter and aspect ratio and thus the microstructure of hot-pressed Si_3N_4 can be controlled by the size distribution and the α/β ratio of the starting powder.

3.3 Sub-Solidus Tie Lines and Known Eutectics

Initial phase studies neglected the SiO_2 content of the Si_3N_4 powder and assumed a simple binary, Si_3N_4/metal oxide, system. Many of these initial results are erroneous. Gauckler and Petzow[34] pointed out that phase relations should be considered in terms of the reciprocal reaction;

$$Si_3N_4 + \frac{6}{x} M_2O_x \rightarrow 3SiO_2 + \frac{4}{x} M_3N_x \quad (3)$$

and thus, for the general case (neglecting impurities and valence changes),

$$zSi_3N_4 + ySiO_2 + \frac{6}{x} M_2O_x \rightarrow (y+3)SiO_2 + \frac{4}{x} M_3N_4 + (z-1)\ Si_3N_4 \rightarrow$$

reaction products (4)

Therefore, the reaction products should be represented in the Si_3N_4-SiO_2-M_2O_x-M_3N_x pseudo-quaternary system (x = metal's valence state).

Compositional changes due to volatilization and the solidification of nitrogen-silicates as glasses are two problems encountered in determining the phase equilibria of Si_3N_4 systems. Because of these and other difficulties, many investigators refer to their results as behavioral diagrams, i.e. indicative of what would be observed using methods of fabricating dense Si_3N_4.

Although different investigators are not in exact agreement, apparent sub-solidus phase relations (i.e. behavioral diagrams) are known for limited, but important compositional areas in the following systems: Si_3N_4-SiO_2-Al_2O_3-ALN,[34,35], Si_3N_4-SiO_2-BeO-Be_3N_2[36,37], Si_3N_4-SiO_2-Al_2O_3-ALN-BeO_2-Be_3N_2,[13] Si_3N_4-SiO_2-Y_2O_3-YN[14,35,39] Si_3N_4-SiO_2-Ce_2O_3-CeN[40], and Si_3N_4-SiO_2-MgO-Mg_3N_2.[15] The latter three, represented by the conventional, partial mole fraction plot, are illustrated in Figs. 2 and 3a. The Si_3N_4-M_3N_x-M_2O_x portion of these three systems are presently unknown.

3.3.1 Si_3N_4-SiO_2-Y_2O_3 System

The Si_3N_4-SiO_2-Y_2O_3 system has been investigated by three groups[14,35,39]. The composition of the apatite phase is still in question. Figure 2a shows the apatite phase with the vacancy composition $Y_9\square(SiO_{3.5}N_{.5})_6\square_2$ which is consistant with the generalized vacancy, site-occupancy/charge balance formula observed for rare-earth, oxy-apatites: $Ln_{8+2x+.67y}(SiO_{4-x}N_x)_6O_y$, where $0<y<2$ and $0<2x+.67y<1.33$. Placement of the nitrogen in the tetrahedral sites is consistant with Morgan's bonding studies for nitrogen-apatites.[41]

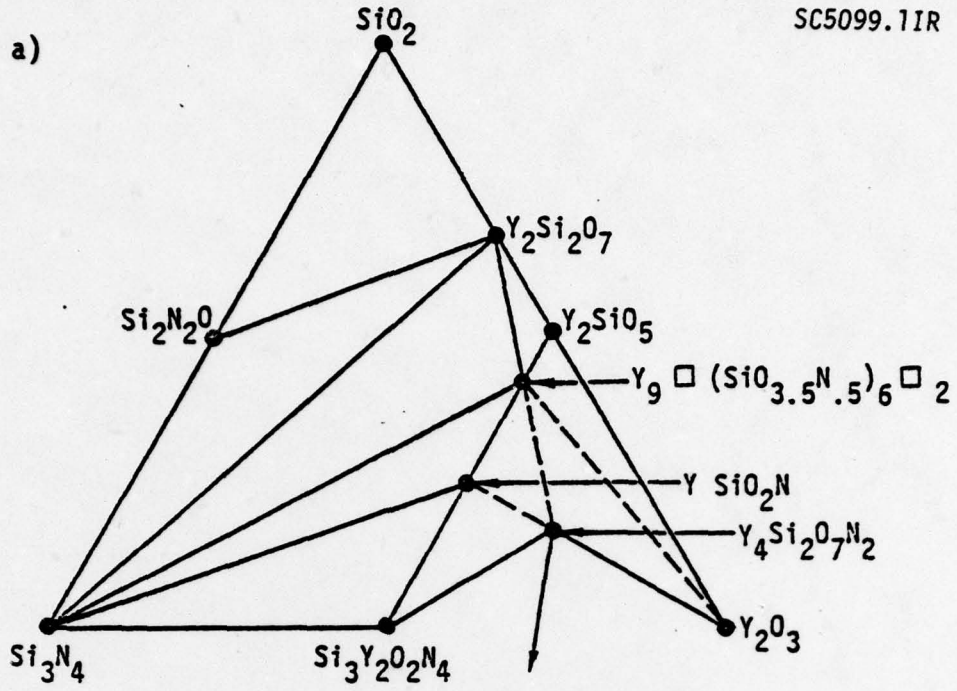

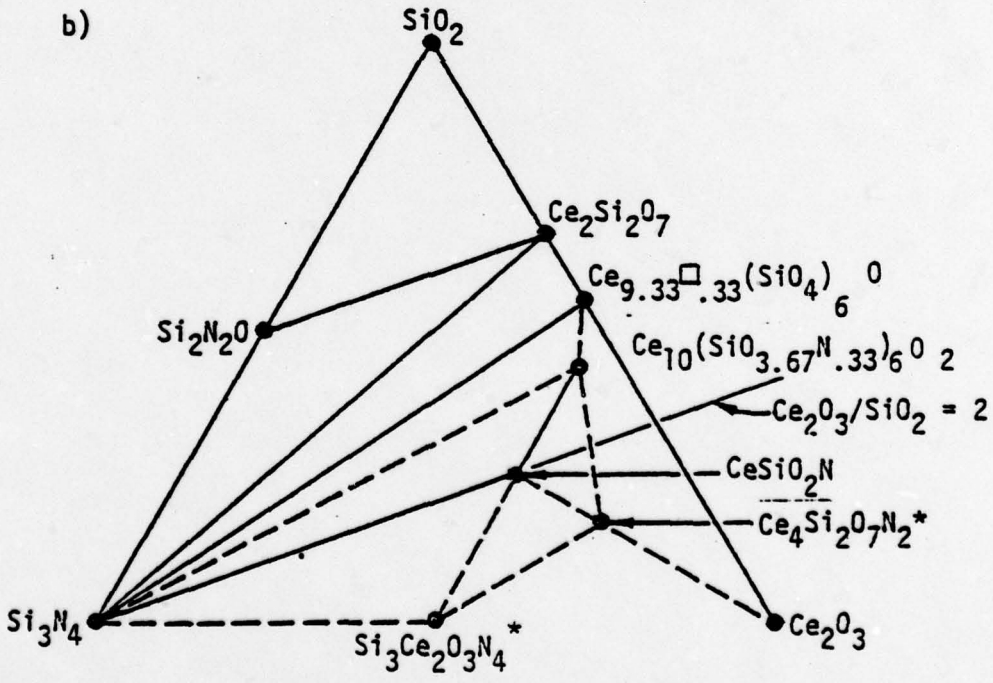

*(expected, but unobserved)

FIGURE 2

a)

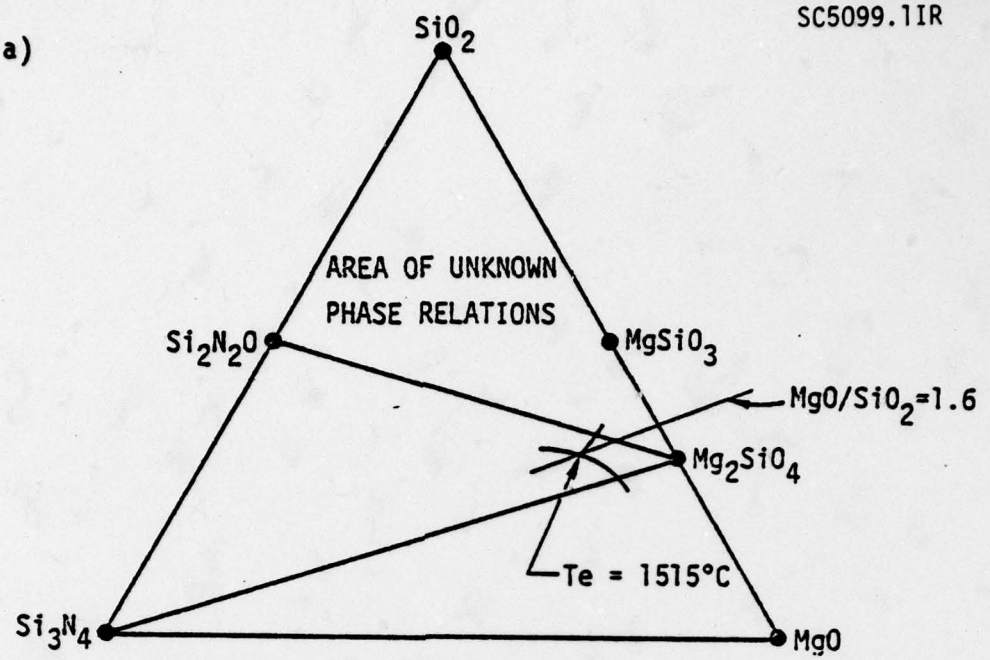
SiO_2
AREA OF UNKNOWN
PHASE RELATIONS
Si_2N_2O
$MgSiO_3$
MgO/SiO_2=1.6
Mg_2SiO_4
Te = 1515°C
Si_3N_4
MgO

b)

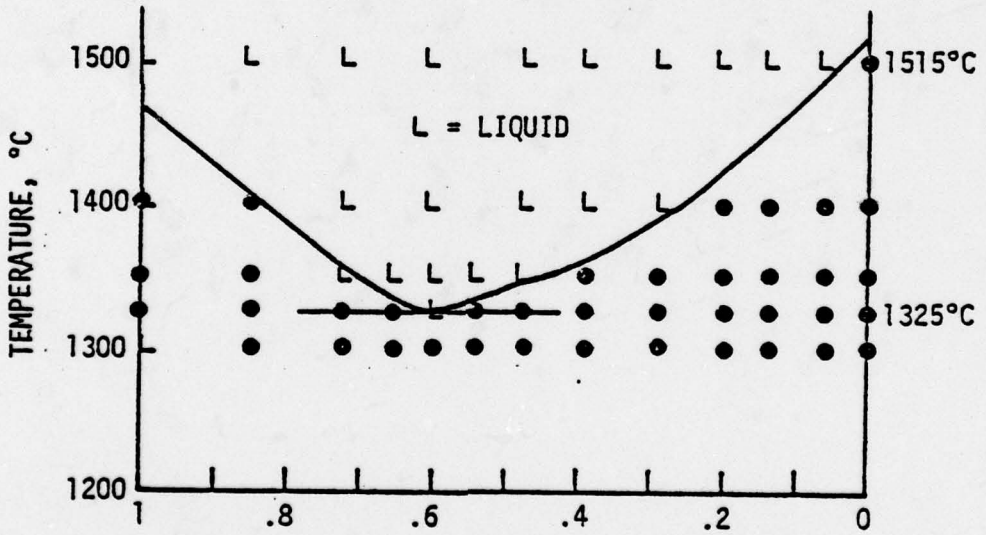
1500
1400
1300
1200
TEMPERATURE, °C
L = LIQUID
1515°C
1325°C
1
.8
.6
.4
.2
0
MOLE FRACTION CaO
IN
0.11 Si_3N_4 + 0.34SiO_2 + 0.55 (MgO, CaO)

FIGURE 3

3.3.2 Si_3N_4-SiO_2-Ce_2O_3 System

Compositions in the Si_3N_4-SiO_2-Ce_2O_3 system can be obtained by the generalized reduction/oxidation reaction:(40)

$$12CeO_2+ySiO_2+zSi_3N_4 \rightarrow 6Ce_2O_3+(3+y)SiO_2+(z-1)Si_3N_4+2N_2 \rightarrow \text{reaction products} \quad (5)$$

In this case, the CeO_2 is reduced to Ce_2O_3 and the oxygen released during this reduction oxidizes some Si_3N_4 to SiO_2. Thus, the use of CeO_2 limits the composition of the products to Ce_2O_3/SiO_2 molar ratios < 2. Due to this compositional limit, the two expected phases (based on an analogy with the Si_3N_4-SiO_2-Y_2O_3 system), $Ce_2Si_3N_4O_3$ and $Ce_4Si_2O_7N_2$ have not been fabricated. The compound $CeSiO_2N$, has the same crystal structure observed for $YSiO_2N$.(42) The exact composition of the nitrogen apatite, represented in Fig. 2b as $Ce_{10}(SiO_{3.67}N_{.33})_6O_2$ ($=Ce_5(SiO_4)_3N$) is still in question.

3.3.3 Si_3N_4-SiO_2- MgO System

The sub-solidus phase relations for the Si_3N_4 SiO_2-MgO system is shown in Fig. 3a. Recent melting experiments(43) have established three important eutectics in this system: 1) the Si_3N_4-Mg_2SiO_4 binary eutectic composition, 0.2 Si_3N_4 + 0.8 Mg_2SiO_4 at 1560°C, 2) the Si_2N_2O-Mg_2SiO_4 binary eutectic composition, 0.4 Si_2N_2O + 0.6 Mg_2SiO_4 at 1525°C, and 3) the Si_3N_4-Si_2N_2O-Mg_2SiO_4 ternary composition, 0.1 Si_3N_4 + 0.3 Si_2N_2O + 0.6 Mg_2SiO_2 at 1515°C.

In addition, the effect of CaO on lowering the ternary eutectic melting temperature has been investigated.(43) This work, summarized in Fig. 3b, was performed by mixing the ternary eutectic with a similar Si_3N_4-Si_2N_2O-Ca_2SiO_4 composition and determining melting temperatures for the composite powders. As illustrated in Fig. 3b, at temperatures >1325°C, a liquid should be present in dense compositions within the Si_3N_4-Si_2N_2O-Mg_2SiO_4 compatibility triangle when CaO is present as an impurity.

4. PROPERTIES: RELATIONS TO COMPOSITION

4.1 Mechanical Properties

The need for α-Si_3N_4 powders to develop the fibrous microstructure important for high toughness and strength has already been discussed above (Section 3.2). The development of the fibrous grain structure under an applied axial pressure during hot-pressing leads to texturing,(27) viz, a greater proportion of the fibers are aligned perpendicular to the hot-pressing direction. All bulk properties exhibit anisotropy caused by

texturing, e.g. flexural strengths are ~20% greater for bar specimens cut perpendicular to the hot-pressing direction relative to parallel specimens.[27]

Mechanical property degradation occurs at high temperatures.[44] The temperature where degradation begins depends on composition. Three compositional effects are known. Historically, the effect of impurities was observed first.[44,45] As clearly demonstrated by Iskoe et al.[46], of the major cation impurities found in Si_3N_4, Ca produces the most significant degradation for material densified with the aid of MgO. The second compositional effect is that due to changes in the major powder constituents as expressed by the MgO/SiO_2 molar ratio[15] for compositions in the Si_3N_4-SiO_2-MgO system. As illustrated in Fig. 4, the flexural strength at 1400°C for a series of materials containing a fixed molar content of Si_3N_4 exhibits a minimum at MgO/SiO_2 ~2, i.e. for

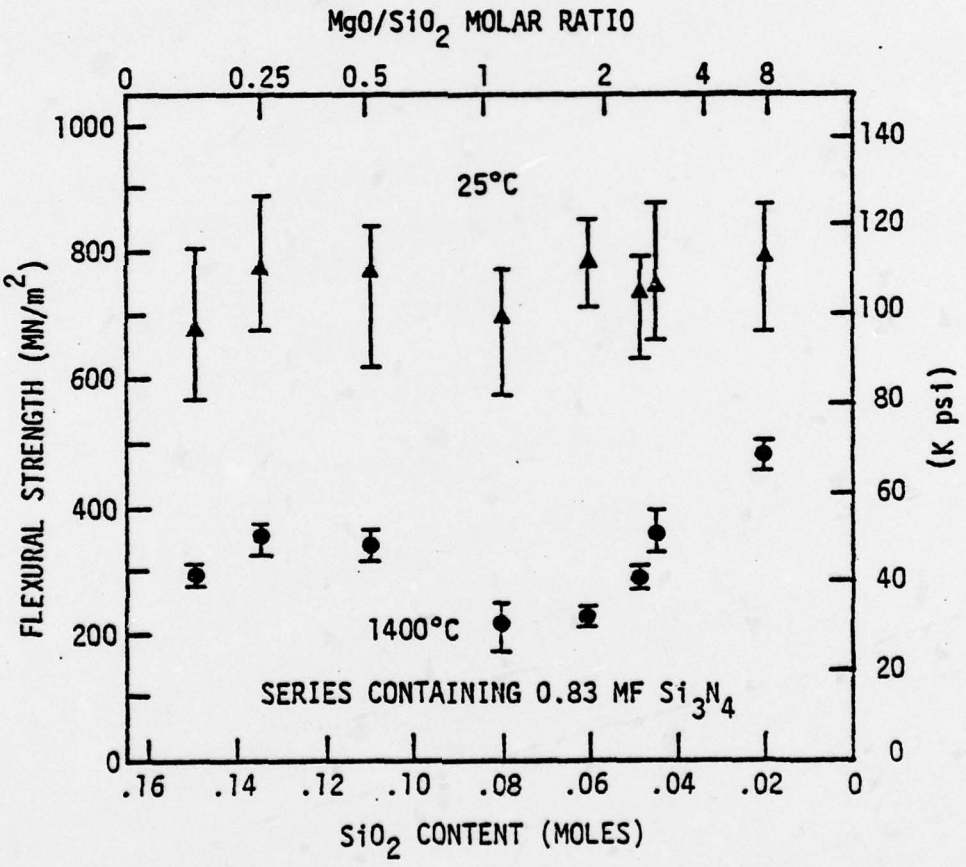

FIGURE 4

compositions close to the Si_3N_4-Mg_2SiO_4 tie line (see Fig. 3a). These data (and similar results obtained for two other series) clearly show the need to know the SiO_2 content, particularly when small amounts of MgO are used for densification. The third compositional effect is caused by major changes in the densification aid, e.g. higher strengths can be obtained at 1400°C for certain compositions within the Si_3N_4-SiO_2-Y_2O_3 and Si_3N_4-SiO_2-Ce_2O_3 systems relative to the compositions that have been fabricated in the Si_3N_4-SiO_2-MgO system.

Many investigators have proposed that the degratation of mechanical properties at high temperature is caused by a viscous liquid located between the elastic Si_3N_4 grains. Models proposed to explain creep and subcritical crack growth indicate that both the viscosity and volume content of the liquid are important parameters.[47] Since a glassy phase is frequently observed at triple points and occasionally between the Si_3N_4 grains,[12] it has been assumed that degradation will begin at a temperature where the glass is soft enough to act as a viscous fluid, e.g. viscosities $<10^7$ poise. This assumption appears consistant with all facts. For example, recent observations have shown that subcritical crack growth (a phenomenon associated with strength degradation in polyphase Si_3N_4) occurs by cavitation and that a tacky phase is observed between the grains associated with extensive cavitation.[48] Since the softening point of a silicate glass is usually ~200°C below its melting temperature, the question of greatest concern is: What is the composition and melting temperature of the glass? An answers to this question might be obtained by studying the phase equilibrium of the relavent system.

Since the eutectic composition solidifies last, it might be expected that the glass composition is close to the eutectic composition. Thus, both the composition and melting temperature of the glass can be approximated by that of the eutectic. If it is assumed that the glass composition is the same as the eutectic, then its volume content can be calculated using the lever rule. With this train of thought, we can now examine what might be expected for compositions in the Si_3N_4-SiO_2-MgO system.

Let us choose a composition in the Si_3N_4-Si_2N_2O-Mg_2SiO_4 compatibility triangle (Fig. 3a) and assume that equilibrium is reached at the fabrication temperature as evident by complete $\alpha \rightarrow \beta$ conversion. During cooling, Si_3N_4 and one of the other two phases will precipitate from the liquid until the eutectic temperature of 1515°C is reached. At this temperature the eutectic liquid is assumed to solidify as a glass. The volume content of this glass will depend on the total composition relative to the eutectic composition. Using the lever rule, it can be shown that the volume of glass is maximum for

FIGURE 5

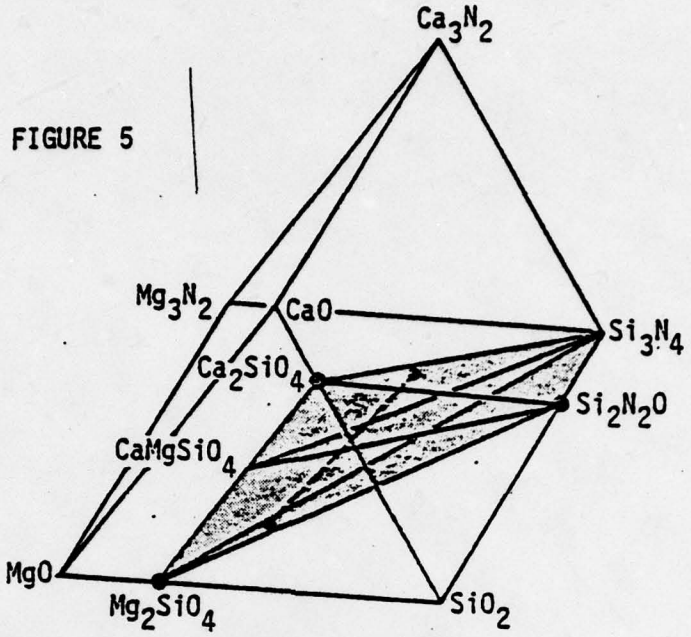

compositions with a MgO/SiO_2 molar ratio of 1.6. If CaO were added as an impurity, the eutectic of interest would lie in the Si_3N_4-Si_2N_2O-Mg_2SiO_4-$CaMgSiO_4$ compatibility element shown in Fig. 5 and the last drop of liquid would not solidify until ~1325°C as shown by the data in Fig. 3b*.

This reasoning can be used to interpret the effects of both impurities and the MgO/SiO_2 ratio on the high temperature strength of compositions within the Si_3N_4-SiO_2-MgO system. Impurities such as CaO will both lower the eutectic temperature and change its composition to promote larger volume contents of the viscous phase. Compositions that exhibit the lowest strength at 1400°C (MgO/SiO_2~2, see Fig. 4) are approximately the same as those that contain the largest amount of viscous phase (MgO/SiO_2=1.6), indicating a close correlation between observed and predicted behavior.

It should be noted that in the absence of a glassy phase a liquid would form at the eutectic temperature. Its volume content will be governed by the lever rule and the temperature above the eutectic. Degradation of mechanical properties as a function of temperature will be more rapid relative to the slow degradtaion observed for materials containing a glass (the viscosity of the glass will decrease as the eutectic temperature is approached, whereas in the absence of a glass, a liquid will not appear until the eutectic temperature). Thus, even in the absence of a glass phase, degradation should be expected above the eutectic temperature.

4.2 Oxidation

The high temperature passive oxidation kinetics of polyphase Si_3N_4 materials can exhibit extreme variations. These variations can be attributed to compositional effects. Three general compositional effects have been observed involving 1) impurities, 2) unstable secondary phases and 3) reactions between the SiO_2 formed during oxidation and the secondary phases.

The effect of impurities can be divided into two categories: homogeneously distributed impurities and hetrogeneously distributed impurities. Oxidation experiments[49] with Si_3N_4 densified with MgO show that the homogeneously distributed impurities such as Ca and Al diffusion from the bulk to the silicate surface scale in an attempt to minimize chemical potential differences. The contamination level within the bulk material can significantly influence the oxidation kinetics as indicated by the different oxidation rates of relatively impure HS110 Si_3N_4 and the purer form of this commercial material manufactured by the Norton Co., NC132 Si_3N_4.[50] Evidence indicates that a portion of the oxide scale was liquid at the oxidation temperature, suggesting that the impurities promote the formation of low temperature eutectics.[49] Hetrogineously distributed impurities in the form of aggregated inclusions of (W,Fe)-silicides rapidly react with the silicate surface scale on Si_3N_4 materials hot-pressed with MgO to form surface pits.[51] These pits can drastically reduce the material's flexural strength.[52] Since a similar reaction is not observed for Si_3N_4 fabricated with Y_2O_3,[51] it can be concluded that the reaction of the Fe with the Si_3N_4-MgO polyphase material produces a low temperature eutectic which locally accelerates the oxidation kinetics to produce a surface pit.

All of the quaternary phases in the Si_3N_4-SiO_2-Y_2O_3 system exhibit non-passive oxidation kinetics, e.g. $Y_2Si_3N_4O_3$ exhibit linear oxidation kinetics.[14] These compounds are unstable in high temperature oxidizing atmospheres relative to Si_3N_4. In addition, all Ce-compounds in the Si_3N_4 SiO_2-Ce_2O_3 system, including the Ce-silicates, oxidize to CeO_2+SiO_2 at relatively low temperatures.[40] The presence of the unstable yittrium phases in polyphase Si_3N_4 can cause considerable material degradation in an elevated temperature regime where Si_3N_4 exhibits very little oxidation, i.e. between 800-1200°C. In this regime, the molar volume change of the oxidized, unstable phases produces surface cracks which exposes more material to oxidation and quickly results in a general dissinegration of the bulk. The Si_3N_4 remains

unoxidized. In this case, the unstable yittrium phases exhibits ~30% increase in molar volume during oxidation. In the Si_3N_4-SiO_2-Ce_2O_3 system, polyphase materials containing small amounts of the unstable Ce-silicate phases do not degrade upon oxidation despite the observed surface oxidation of the unstable phases. For this case, the molar volume increase of the Ce-silicates is ~8%. These observations suggest further studies into the relations between volume changes produced by oxidation and the stress distributions that arise in these polyphase materials.

Of all the polyphase Si_3N_4 materials examined, materials fabricated in the Si_3N_4-Si_2N_2O-$Y_2Si_2O_7$ compatibility triangle (see Fig 2a) exhibit the greatest resistance to oxidation.[14] The apparent reason for this is the compatibility of SiO_2, the oxidation product of Si_3N_4, with the secondary phases, $Y_2Si_2O_7$ and Si_2N_2O, and the relatively high eutectic temperatures within this compositional area. When this compatibility does not exist, as in the Si_3N_4-SiO_2-MgO system (see Fig. 3a), the secondary phases, e.g. Mg_2SiO_4, will take part in the oxidation reaction to form silicates richer in SiO_2 as evident by the $MgSiO_3$ phase observed in the oxide surface scale of Si_3N_4 fabricated with MgO.[49] The diffusivity during the SiO_2-second phase reaction should increase the oxidation kinetics of Si_3N_4 as evident by the decrease in oxidation resistance of materials fabricated with increasing MgO/SiO_2 molar ratios.[15]

5. CONCLUDING REMARKS

It is obvious that phase equilibria is a very powerful tool in understanding the relations between fabrication, microstructure development and properties. In developing these interrelations, all chemical constituents must be considered. For example, it has been shown that small amounts of impurities can produce large effects. Knowing how the material is made is essential in anticipating improvements.

ACKNOWLEDGMENTS

The fabrication section of this work was supported by a Rockwell International Independent Research and Development program. The property section was supported by the Air Force Office of Scientific Research, Contract No. F49620-77-C-0072.

REFERENCES

1. C. Greskovich and H.H. Rosolowski, J. Amer. Ceram. Soc. 59, 337 (1976).
2. S.C. Singhal, Ceramurgia Inter. 2, 123 (1976).
3. F.F. Lange, unpublished work.
4. G.G. Deeley, J.M. Herbert and N.C. Moore, Powder Met. 8, 145 (1961).
5. G.R. Terwilliger and F.F. Lange, J. Mat. Sci. 10, 1169 (1975).
6. L.J. Gaukler, S. Boskovic, I.K. Naik and T.Y. Tien, Proc. Workshop on Ceramics for Adv. Heat Engines, Orlando, Fla., 1977, p. 321, NTIS Conf. 770110, UC95a.
7. H.F. Priest, G.L. Priest and G.E. Gazza, J. Amer. Ceram. Soc. 60, 81 (1977).
8. M. Mitomo, J. Mat. Sci. 11, 1103 (1976).
9. J.V. Sharp and A.G. Evans, J. Mat. Sci. 6, 1292 (1971).
10. R. Kossowsky, J. Mat. Sci. 8, 1603 (1973).
11. P. Drew and M.H. Lewis, J. Mat. Sci. 9, 261 (1974).
12. D.R. Clarke and G. Thomas, J. Amer. Ceram. Soc. (in press).
13. L.J. Gaukler, H.L. Lukas, and T.Y. Tien, Mat. Res. Bull. 11, 503 (1976).
14. F.F. Lange, S.C. Singhal and R.C. Kuznicki, J. Amer. Ceram. Soc. 60, 249 (1977).
15. F.F. Lange, J. Amer. Ceram. Soc., (in press).
16. F.F. Lange, H.J. Siebenneck and D.P.H. Hasselman, J. Amer. Ceram. Soc. 59, 454 (1976).
17. C. Wagner, J. Appl. Phys. 29, 1295 (1958).
18. A. Atkinson, A.J. Moulson and E.W. Roberts, J. Mat. Sci. 10, 1242 (1975).
19. F.F. Lange, Discussion; NATO ASI on Nitrogen Ceramics, Canterbury, England, Aug. 1976, in press.
20. D.R. Messier and P. Wong, J. Amer. Ceram. Soc. 56, 480 (1973).
21. Sin-Shong Lin, J. Amer. Ceram. Soc. 60, 768 (1977).
22. F.F. Lange and J.L. Iskoe, unpublished work.
23. D. Hardie and K.H. Jack, Nature 180, 332 (1957).
24. R. Marchand, Y. Laurent, J. Lang and M.T. LeBihan, Acta Crys. 25, 2157 (1969).
25. I. Kohatsu and J.W. McCauley, Mat. Res. Bull. 9, 917 (1974).
26. K. Kato, Z. Inque, K. Kiljima, I. Kawada, H. Tanaka and T. Yanane, J. Amer. Ceram. Soc. 58, 90 (1975).
27. F.F. Lange, J. Amer. Ceram. Soc. 56, 518 (1973).
28. A. Atkinson and A.D. Evans, Trans. and J. Brit. Ceram. Soc. 73, 43 (1974).
29. F.F. Lange, "Task I: fabrication, Microstructure and Properties of Selected SiAlON Compounds", Final Report, NAVAIR Systems. N00019-73-C-0208, Feb. 1974.

30. H.R. Baumgartner and D.W. Richerson, Fracture Mechanics of Ceramics, Vol. 1, p. 367, Ed. by R.C. Bradt, D.P.H. Hassleman and F.F. Lange, Plenum, 1974.
31 G.R. Terwilliger and F.F. Lange, J. Amer. Ceram. Soc. 57, 25 (1974).
32. R.J. Brook, T.G. Carruthers, L.J. Bowen and R.J. Weston, Proc. NATO ASI on Nitrogen Ceramics, in press.
33. J.L. Iskoe and F.F. Lange, Proc. Mircostructure of Ceramics, Berkely, Aug. 1976 (in press).
34. L.J. Gauckler, H.L. Lukas and G. Petzow, J. Amer. Ceram. Soc. 53, 346 (1975).
35. K.H. Jack, J. Mat. Sci. 11, 1135 (1976).
36. I.G. Huseby, H.L. Lukas and G. Petzow, J. Amer. Ceram. Soc. 58, 377 (1975).
37. D.P. Thompson and L.J. Gauckler, J. Amer. Ceram. Soc. 60, 470 (1977).
38. D.P. Thompson, J. Mat. Sci. 11, 1377 (1976).
39. R.R. Wills, S. Holmquist, J.M. Wimner and J.A. Cunningham, J. Mat. Sci. 11, 1305 (1976).
40. F.F. Lange, "Fabrication of Si_3N_4-Ce_2O_3-SiO_2 Materials: Phase Relations, Sinterability, Strength and Phast Stability", to be pub.
41. P.E.D. Morgan, Bull. Amer. Ceram. Soc. 56, 300 (177).
42. P.E.D. Morgan, P.J. Carroll and F.F. Lange, Mat. Res. Bull. 12, 251 (1977).
43. F.F. Lange, unpublished work.
44. F.F. Lange, J. Amer. Ceram. Soc. 57, 84 (1974).
45. D.W. Richerson, Bull. Amer. Ceram. Soc. 52, 560 (1973).
46. J.L. Iskoe, F.F. Lange and E.S. Diaz, J. Mat. Sci. 11, 908 (1976).
47. F.F. Lange, Deformation of Ceramic Materials, p. 361, Ed. by R.C. Bradt and R.C. Teressler, Plenum Press, 1975.
48. F.F. Lange, "Evidence for Cavitation Carck Growth in Si_3N_4," to be submitted for publication.
49. S.C. Singhal, J. Mat. Sci. 11, 500 (1976).
50. A.F. McLean, E.A. Fisher and R.J. Bratton, Brittle Materials Design, High Temperature Gas Turbine, Interim Report AMMRC-CTR-72-19, p. 158, Sept. 1972.
51. F.F. Lange, "Reaction of Iron with Si_3N_4 Materials to Produce Surface Pitting," to be published.
52. S.C. Singhal, "Effects of Oxidation on Strength Reduction in Si_3N_4 and SiC," to be published.

SECURITY CLASSIFICATION OF THIS PAGE (When Data Entered)

REPORT DOCUMENTATION PAGE

READ INSTRUCTIONS BEFORE COMPLETING FORM

1. REPORT NUMBER: AFOSR-TR- 78-0943
2. GOVT ACCESSION NO.:
3. RECIPIENT'S CATALOG NUMBER:

4. TITLE (and Subtitle): High Temperature Mechanical Properties of Polyphase Ceramics Based on Si_3N_4

5. TYPE OF REPORT & PERIOD COVERED: Interim 02/01/77 - 01/31/78

6. PERFORMING ORG. REPORT NUMBER: SC5099.1IR

7. AUTHOR(s): F. F. Lange

8. CONTRACT OR GRANT NUMBER(s): F49620-77-C-0072 New

9. PERFORMING ORGANIZATION NAME AND ADDRESS:
Rockwell International Science Center
1049 Camino Dos Rios
Thousand Oaks, CA 91360

10. PROGRAM ELEMENT, PROJECT, TASK AREA & WORK UNIT NUMBERS: 61102F, 2306/A2

11. CONTROLLING OFFICE NAME AND ADDRESS:
Major W. C. Simmons
Air Force Office of Scientific Research / NE
Bolling AFB, D.C. 20332

12. REPORT DATE: March, 1978

13. NUMBER OF PAGES: 76

14. MONITORING AGENCY NAME & ADDRESS (if different from Controlling Office):

15. SECURITY CLASS. (of this report): UNCLASSIFIED

15a. DECLASSIFICATION/DOWNGRADING SCHEDULE:

16. DISTRIBUTION STATEMENT (of this Report)

Approved for public release; distribution unlimited.

17. DISTRIBUTION STATEMENT (of the abstract entered in Block 20, if different from Report)

18. SUPPLEMENTARY NOTES

19. KEY WORDS (Continue on reverse side if necessary and identify by block number)

Silicon nitride	Phase Equilibrium	Oxidation
Creep	Eutectics	
Cavitation	Strength	
Slow Crack Growth	Fracture	

20. ABSTRACT (Continue on reverse side if necessary and identify by block number)

Progress is summarized in the following study areas: (1) eutectic studies in the Si_3N_4- MgO-SiO_2 system relating eutectic compositions and temperatures to fabrication, microstructure and mechanical properties; (2) evidence for high temperature cavitation crack growth in polyphase Si_3N_4 materials; (3) estimates of the time required for the stress induced penetration of a liquid from triple points to locations between grains; (4) the reaction of Fe with polyphase Si_3N_4 to form surface pits during oxidation which lead to strength degradation, (5) creep behavior of polyphase Si_3N_4/MgO alloys in relation to

DD FORM 1 JAN 73 1473 EDITION OF 1 NOV 65 IS OBSOLETE

UNCLASSIFIED

SECURITY CLASSIFICATION OF THIS PAGE (When Data Entered)